GigaScience

Defining the characteristics of interferon-alpha-stimulated human genes: insight from expression data and machine-learning

--Manuscript Draft--

Manuscript Number:	GIGA-D-22-00042R1
Full Title:	Defining the characteristics of interferon-alpha-stimulated human genes: insight from expression data and machine-learning
Article Type:	Research
Funding Information:	Medical Research Council (MC_UU_1201412) — Prof David L. Robertson China Scholarship Council (201706620069) — Mr Haiting Chai
Abstract:	Background: A virus-infected cell triggers a signalling cascade resulting in the secretion of interferons (IFNs). It in turn induces the up-regulation of the IFN stimulated genes (ISGs) that play anti-pathogen roles in host defenses. Here, we conducted analyses on large-scale data relating to evolution, gene expression, sequence compositions, and network properties to elucidate factors associated with the stimulation of human genes in response to the typical IFN-α. Results: We propose that the ISGs are less evolutionary conserved than genes that are not significantly stimulated in IFN experiments (non-ISGs). ISGs show obvious depletion of GC-content in the coding region, leading to differential representations in their sequence compositions. The IFN repressed human genes (IRGs), which are down-regulated in IFN experiments can have similar properties to the ISGs. Additionally, we also design a machine-learning framework integrating the support vector machine and novel feature selection algorithm. It achieves an area under the receiver operating characteristic curve (AUC) of 0.7455 for the ISG prediction and demonstrates the similarity between the ISGs triggered by type I and III IFNs. Conclusions: The ISGs have unique properties that make them different from the non-ISGs. Some of them have strong correlations with genes' expression following IFN-α stimulations. which can be used as good features in machine learning. Our model predicts several genes as potential ISGs that so far have shown no significant differential expression when stimulated with IFN-α in the cell/tissue types in the available databases. A webserver implementing our method is accessible at http://isgpre.cvr.gla.ac.uk/ . The docker image at https://hub.docker.com/r/hchai01/isgpre can be downloaded to reproduce the analysis.
Corresponding Author:	Joseph Hughes University of Glasgow Centre for Virus Research Glasgow, Glasgow UNITED KINGDOM
Corresponding Author Secondary Information:	
Corresponding Author's Institution:	University of Glasgow Centre for Virus Research
Corresponding Author's Secondary Institution:	
First Author:	Haiting Chai
First Author Secondary Information:	
Order of Authors:	Haiting Chai Quan Gu David L. Robertson Joseph Hughes
Order of Authors Secondary Information:	

Response to Reviewers:	Comments from Reviewer #1: In this manuscript, the authors analyzed different characteristics that are potentially related to the expression of human genes under IFN-a stimulation. A classification model is built to predict ISG (genes that are upregulated following IFN-a stimulation) from the human fibroblast cell. The model also performs feature selection, and the authors used different test sets (on different types of IFN) to validate their model. The authors provide a web server that implemented this machine learning model. ---------- Key comment 1: I liked the introduction, the background and motivation were clear. However, the Results section was a bit hard to follow, in particular the implementation of the machine learning models, with different classifiers applied inconsistently across distinct feature sets. Our reply: Thanks for the suggestions. We have changed the structure of the results section and added some appendices to enhance the readability of our manuscript. Table 3 now includes two main parts: 1) comparison of different machine learning methods (KNN, RF and SVM); 2) comparison of SVM classifiers optimised by different feature selection strategies (FFS and ASI); Due to the rationale behind random forest, the final number of features shown in Table 3 is not 518. The result of the first comparison proves the effectiveness of SVM. The result of the second comparison proves the effectiveness of our feature selection strategy (see Figure 15). We have amended the structure of Table 3 to make it more understandable. ---------- Key comment 2: Regarding reproducibility, the authors provide a Github repository with source code, the model trained and data. From the documentation and notes in the manuscript (lines 1015-1023), looks like this can only be run on mac OS, which makes it very hard for me to test (I'm a Linux user). I recommend the authors to read and follow the article "Reproducibility standards for machine learning in the life sciences" (https://doi.org/10.1038/s41592-021-01256-7). Having, for instance, a Docker image to download and run your analyses would be fantastic. Our reply: Thanks for your comments. We have added a Docker implementation for our machine learning method. The image is available at https://hub.docker.com/r/hchai01/isgpre. Instructions can be found at our GitHub repository (https://github.com/HChai01/ISGPRE). ---------- Key comment 3: The authors perform a comprehensive analysis of features that differentiate different gene classes. I wonder why didn't they use first a machine learning model to automatically find these important features, and then try to analyse which features were selected (instead of the other way around as done in the study). I think there is perhaps too much manual feature engineering in the previous steps of training an ML model. Our reply: Thanks for the comment. The analyses and machine learning are separated in our project. In the analyses, we aim to find as many ‘important’ features as possible but in the machine learning, we aim to find an optimal way to classify the considered classes with limited information. It should be noted that some samples used for feature analyses were not included in the training or modelling stage as they were randomly selected for independent testing (see the newly added Figure 2). Such random sampling procedures will change the distribution of the features, especially those for the major class (non-ISGs), which means the feature processed in the machine learning stage is not the same as the one used in the analysis stage. In other word, the feature distribution of samples used for training can’t truly reflect the natural distribution of the considered classes. Some key insights may be missed if we first use machine learning models to find ‘important’ features for later analyses. Lastly, we have optimised our machine learning pipeline to make it easy to follow. ---------- Key comment 4: Related to the previous point, in my comments below one of my

concerns is about feature correlation. The authors compare individual features regarding their ability to separate different gene classes (ISG vs background vs non-ISG). But one can imagine that some features are highly correlated. Some features might not be useful to separate gene classes from a single-feature analysis (as the authors do at the beginning), but they could be useful in combination with other features. Unless I'm missing an important point, I would leave the machine learning model to learn this and then analyze each feature individually after the model identifies them.

Our reply: Yes, you are right. The combination of some features can contribute to separate gene classes. Machine learning models do help to identify this. Features with high importance in machine learning have a higher chance to have differential distribution in nature but it is not guaranteed due to random sampling. On the other hand, features with better discrimination in analyses may have a higher chance to enhance the quality of the machine learning model but it is also not guaranteed (see Figure 9-11 & Table 4). The clues shown in both analyses and machine learning can further highlight some features that make a gene stimulated under IFN-alpha. However, it is not a good reason to ignore the contribution of some features in identifying ISGs just because they are not performing well in the machine learning stage. It is acceptable to put the machine learning before or after the feature analyses. We put feature analyses first because this paper is mainly focused on finding out what changes the expression of a human gene following IFN-alpha stimulation. Machine learning is our strategy to see if some features can be used to identify ISGs in a high-throughput way.

Key comment 5: Authors are concerned that including too many features in the support vector machine (SVM) model would complicate the prediction task. To remedy this, they manually select the features according to, in my opinion, a more subjective criterion. Why didn't the authors use a feature selection algorithm here? I know that they propose a model including feature selection, but I guess I don't understand well all the previous manual feature analyses. Using a known feature selection method here would provide a more data-driven approach to improve classification, in addition to their manual expert curation (which is also valid).

Our reply: Thanks for the suggestion. We have added the comparison among different feature selection strategies to prove the effectiveness of ours.

Key comment 6: They run several classification models, but not consistently across the same set of features. For example, only SVM is run across genetic, parametric, all features, etc, but not the other models. Why is that?

Our reply: Thanks for the comments. As previously mentioned, the comparisons shown in Table 3 first identify which base machine learning method performs best. We then use the best-performing method (SVM) to test the performance of different feature sets. We have amended the structure of Table 3 to make it easier to understand.

Key comment 7: The manuscript would really benefit from a figure with the main steps of the analyses performed, models tested, datasets employed, etc. It's hard to get the big picture as it is now.

Our reply: Thanks for your suggestion. We have added a figure to show this (see new Figure 2).

Key comment 8: I think the window size used (mentioned in the text) should be added to the Figure 2 caption.

Our reply: Thanks for your suggestion. We have added it to the caption (see new Figure 3).

Key comment 9: * What's the vertical dashed line? In the text, you say that those at the left of this line are IRGs, but I don't understand the meaning of that vertical line (-0.9 log fold change). This explanation, which I didn't see, should be added to the figure caption also.

Our reply: Thanks for the comment. In our collected data, the log fold change of IRGs are all lower than -0.9. That's why we mentioned 'that those at the left of this line are IRGs'. We have updated the figure and divided each plot into three regions. All data points in the left region come from IRGs (Log2(FoldChange) < -0.871); points in the right region all come from ISGs (Log2(FoldChange) > 0.686); points in the middle region may come from ISGs or non-ISGs (including IRGs).

Key comment 10: From the text, I understand that in the subfigures in Figure 2 you have IRGs, non-ISGs and ISGs. Would it be possible, or meaningful for the reader, to add an extra vertical line to separate them?

Our reply: Thanks for the comment. Current vertical line (x=-0.871) is used to separate some but not all IRGs. We have added a new vertical line to separate some ISGs (x=0.686). However, the source of data points in the region between x=–0.871 and x=0.686 are complex. They may come from ISGs or non-ISGs (including IRGs). We have added some description in the figure caption.

Key comment 11: If GC-content is underrepresented in ISGs more than non-ISGs, the ApT and TpA should be expected to be more enriched in ISGs, right? Sounds like a redundant analysis. I would expect these two sequence-derived features to be correlated. If this is the case, maybe it would be better to highlight other features instead of a correlated/expected one?

Our reply: Thanks for the suggestion. The depletion of GC-content in ISGs has some impacts on the representation of dinucleotide composition, codon usages and amino acid composition. We expect the representations of some GC-related features may be underrepresented but we cannot tell more unless those features were analysed. For instance, it's hard to tell whether the depletion of CpG or GpC is more important to the stimulation of human genes under IFN-alpha. Therefore, these analyses are not redundant as long as they are not completely the same (e.g., GC-content, CG-content or AT-content).

Key comment 12: Figure 4: here the authors divided the parametric set of features into four categories and compared their representations among ISGs, non-ISGs and background genes. The figure shows p-values of the tests on the y-axis, and the four categories of features on the x-axis. I think it's important to run a negative control: could you please run these tests again, say, 100 times, with gene IDs/names shuffled, and check whether some of these results also appear in these null simulations? Maybe you can keep the same figure but remove those also found in the null simulations.

Our reply: Thanks for the comments. First of all, the red squares in this figure (now Figure 5) show the comparisons of some genome-based features between the stimulated class (ISGs) and non-stimulated class (non-ISGs). The blue triangles are also placed in the same figure as the restriction of filtering 'high confident' non-ISGs may also have some impacts to form a 'special' distribution differential to ISGs'. We figure that the negative control may not be helpful here as the features we analysed are all inherent thus will not change due to the impact of IFN-treatment. We do have some samples with almost invisible changes in the experiments. They are called ELGs and the comparison between ELGs and ISGs are shown in Figure 11. We have updated the caption of the figure to make it easier to understand.

Key comment 13: Is it possible that the comparison of codons frequencies (third category of features) is correlated with previous findings (like GC content or ApT/TpA enrichment)? If so, would it be possible that maybe the analysis is also expected or redundant? For example, in ISGs there is an underrepresentation of GC-content, and

you also found that ISGs there is an underrepresentation of "CAG" codons. I might be missing something, but aren't these expected to be correlated?

Our reply: Yes, you are right. The codon usages are influenced by the nucleotide composition in the CDs. The analysis can be expected but is not redundant. As we mentioned in the reply to your key comment 11, we aim to have better understanding of each feature rather than expecting that they are over- or under-represented in ISGs.

Key comment 14: Figure 6: I would suggest adding the same negative control suggested before.

Our reply: Thanks for the comments. We believe the negative control may not be helpful here as the representation of features are not influenced by the IFN experiments.

Key comment 15: I think it's important to define what are all those eight features in the network analyses (closeness, betweenness, etc), otherwise it's hard to follow what comes next.

Our reply: Yes, you are right. We have already provided this information in the Method Section: ‘Generation of discrete features’. Please check the last paragraph of that section for details.

Key comment 16: Figures 9 and 10: it would be good to add the sign of the correlation in the figure, in addition to mentioning it in the caption (as it is now).

Our reply: Thanks for your suggestion. We have corrected the figure about negative correlation (see new Figure 11). The sign now can be found in the y-axis. We have also added some description in the figure caption. Please check new Figure 10/11 for details.

Key comment 17: Given the unique patterns or differences between non-ISG class and IRG class, wouldn't it be better to perform different analyses excluding IRG genes? The authors also acknowledge these risks in lines 539-541.

Our reply: Thanks for your suggestion. However, the main focus of the current paper is to identify what makes a human gene stimulated in the presence of IFN-alpha. The investigation of IRGs is a side analysis to show that it does not influence the definition of a ‘null stimulation’.

Key comment 18: It was hard for me to understand the workflow in this section: you used different machine learning models applied to distinct features sets, for example. Why don't you apply the same set of models to the same set of features? I think this section needs an initial paragraph with a global description of what you are trying to do.

Our reply: Thanks for your suggestion. The workflow in this section is: 1) find the best-performed base method; 2) find the optimal feature set; 3) train the machine learning model with the best-performing base method and optimal feature set. The final model is then used for testing the 7 test datasets mentioned in Table 5. We have added a global description at the beginning of this section to make it easier to follow.

Key comment 19: For example, I don't think I understand very well the concept of "disruptive feature". What does it mean?

Our reply: Thanks for the comments. A feature is identified as ‘disruptive’ if the overall performance of the classifier becomes worse after being added. We have changed it to ‘noisy’ in the hope that this is more understandable.

Key comment 20: Table 3: I don't understand the threshold selection here. I guess you refer to classification or decision threshold from a model that outputs a probability of a gene to be ISG or non-ISG. First, I think there should be a line separating each performance measure to clearly show those that are "Threshold-dependent" and "Threshold independent"

Our reply: Yes, you are right. Thanks for the suggestion. We have added a line to separate the threshold-dependent and threshold-independent criteria.

Key comment 21: I also understand that, during cross-validation, you selected for each model/feature set combination, the threshold that maximized the MCC (this is explained in Table 3 as a footnote, but it should be more explicitly mentioned in the text).

Our reply: Thanks for the suggestion. We have added some description for it.

Key comment 22: Table 3: What is the "Optimum" set of features? Why is this "Optimium set" only used with SVM?

Our reply: Thanks for the comments. The ‘optimum’ set of features are generated via our feature selection scheme (Figure 16). The workflow in this section is first identify the best-performing machine learning method then use it (SVM) with the feature selection strategy to identify the ‘optimal’ feature set (No.=74). We have added some further description in the footnote of Table 3.

Key comment 23: How does the "AUC-driven subtractive iteration algorithm (ASI)" compare with other feature selection algorithms.

Our reply: Thanks for the comments. Our feature selection method is developed based on the ‘Backward Feature Elimination’ scheme. We have compared it with another important Sequential Feature Selection method: ‘Forward Feature Selection’ scheme. Please check Table 3 and Results section: ‘Implementation with machine learning framework’ for details.

Key comment 24: Table 5: you mention this in the text, but it would be good to have an extra column indicating which datasets were used for training and which are for testing.

Our reply: Thanks for the suggestion. We have reshuffled the structure of Table 5 to make this clear.

Key comment 25: Figure 13: it would be good to have the AUROC in the figure, not only the curves.

Our reply: Thanks for the suggestion. We have added 'ROC' note in Figure 13.

Comments from Reviewer #2:
First of all, this manuscript is well-written after a thorough research investigation. I enjoyed reading about interferons, interferon stimulating genes (ISGs), mechanisms and signalling pathways. In the introduction, the authors have highlighted the different methods (including other bioinformatics databases) available to identify ISGs and their potential pitfalls. This unmet need is addressed using in silico approaches which were used to classify interferon stimulating genes from non-stimulating ones in human fibroblast cells. Here, the authors have applied a combination of expression data and sequential/compositional features and designed a machine learning model for the prediction of ISGs from non-ISGs.

	Apart from features like duplication, alternative splicing, mutation and presence of multiple ORFs, the authors extracted various sequential features and found them to be correlated well with ISG prediction. For example, ISGs are prone to GC depletion and a significant difference in the codon usage among ISGs was found. In that context, the authors claim that ISGs are evolutionarily less conserved, codon usage features, genetic composition features, proteomic composition features and sequence patterns (especially like SLNPs and SLAAPs) are optimal parameters that can cumulatively help in differentiating ISGs from non-ISGs. When it comes to building a machine learning model, the authors faced challenges due to similarities between ISGs and IRGs. They have experimented using different algorithms for model building ranging from the decision tree, and random forest and found decent results with support vector machine. Key comment 1: Model Prediction accuracy was close to 70% for type I and III IFN and it performed below par when it comes to predicting ISGs activated by type II IFN system. There is scope to improvise the model prediction accuracy and extend its usage to type II IFN systems. If the authors could briefly add few points on how to improve the model accuracy and also highlight the application/impact of this work in their discussion, that would help scientists from other background to resonate with this manuscript. Our reply: Thanks for the suggestion. We have added some points on how to improve the model accuracy and highlighted the application/impact of this work in the discussion section.
Additional Information:	
Question	Response
Are you submitting this manuscript to a special series or article collection?	No
Experimental design and statistics Full details of the experimental design and statistical methods used should be given in the Methods section, as detailed in our Minimum Standards Reporting Checklist. Information essential to interpreting the data presented should be made available in the figure legends. Have you included all the information requested in your manuscript?	Yes
Resources A description of all resources used, including antibodies, cell lines, animals and software tools, with enough information to allow them to be uniquely identified, should be included in the Methods section. Authors are strongly encouraged to cite Research Resource Identifiers (RRIDs) for antibodies, model	Yes

organisms and tools, where possible. Have you included the information requested as detailed in our Minimum Standards Reporting Checklist?	
Availability of data and materials All datasets and code on which the conclusions of the paper rely must be either included in your submission or deposited in publicly available repositories (where available and ethically appropriate), referencing such data using a unique identifier in the references and in the “Availability of Data and Materials” section of your manuscript. Have you have met the above requirement as detailed in our Minimum Standards Reporting Checklist?	Yes

Defining the characteristics of interferon-alpha-stimulated human genes: insight from expression data and machine-learning

Haiting Chai[1], Quan Gu[1], David L. Robertson[1,*], Joseph Hughes[1,*]

[1]MRC-University of Glasgow Centre for Virus Research, Glasgow, United Kingdom

*david.l.robertson@glasgow.ac.uk, joseph.hughes@glasgow.ac.uk

Abstract

Background: A virus-infected cell triggers a signalling cascade resulting in the secretion of interferons (IFNs), which in turn induces the up-regulation of the IFN stimulated genes (ISGs) that play a role in anti-pathogen host defence. Here, we conducted analyses on large-scale data relating to evolutionary, gene expression, sequence composition, and network properties to elucidate factors associated with the stimulation of human genes in response to IFN-α.

Results: We find that ISGs are less evolutionary conserved than genes that are not significantly stimulated in IFN experiments (non-ISGs). ISGs show obvious depletion of GC-content in the coding region. This influences the representation of some compositions following the translation process. IFN repressed human genes (IRGs), down-regulated genes in IFN experiments, can have similar properties to the ISGs. Additionally, we design a machine-learning framework integrating the support vector machine and novel feature selection algorithm that achieves an area under the receiver operating characteristic curve (AUC) of

0.7455 for ISG prediction. Its application in other IFN-systems suggests the similarity between the ISGs triggered by type I and III IFNs.

Conclusions: ISGs have unique properties that make them different from the non-ISGs. Some properties have strong correlations with genes' expression following IFN-α stimulations, which can be used as predictive features in machine learning. Our model predicts several genes as putative ISGs that so far have shown no significant differential expression when stimulated with IFN-α in the cell/tissue types in the available databases. A webserver implementing our method is accessible at http://isgpre.cvr.gla.ac.uk/. The docker image at https://hub.docker.com/r/hchai01/isgpre can be downloaded to reproduce the prediction.

Key words: anti-viral response, interferon, interferon stimulated genes, omics data analyses, machine-learning.

Introduction

Interferons (IFNs) are a family of cytokines defined for their capacity to interfere with viral replication. They are secreted from host cells after an infection by pathogens such as bacteria or viruses to trigger the innate immune response with the aim of inhibiting viral spread by 'warning' uninfected cells [1]. The response induced by IFNs is rapid and feedforward, to synthesize new IFNs, which guarantees a full response even if the initial activation is limited [2]. In humans, several IFNs have been discovered (e.g. IFN-α/β/ε/κ/ω/γ/λ [3-8]). IFN-α, IFN-β, IFN-ε, IFN-κ, IFN-ω are grouped into type I IFNs for signalling through the common IFN-α receptor (IFNAR) complex present on target cells [3-6] (**Figure 1A**). IFN-α comprises 13 subtypes in humans while the remaining type I IFNs are encoded by a specific gene [9]. IFN-λ targets IFN-λ receptor 1 (IFNLR1)/interleukin-10 receptor 2 (IL-10R2) and was classified as

type III IFN following its discovery in 2003 [8] (**Figure 1C**). Similar to type I IFNs, IFN-λ also exert antiviral properties but functions less intensely [10-12]. IFN-γ is classified as type II IFN and manifests its biological effects by interacting with IFN-γ receptor (IFNGR) [7] (**Figure 1B**). In contrast to type I and III IFNs, IFN-γ is also anti-pathogen, immunomodulatory, and proinflammatory but more focused on establishing cell immunity [3,7,11,13].

All three types of IFNs are capable of activating the Janus kinase/signal transducer and activator of transcription (JAK-STAT) pathway and inducing the transcriptional up-regulation of approximately 10% of human genes that prime cells for stronger pathogen detections and defenses [9,14,15]. These up-regulated human genes are referred to as IFN-stimulated genes (ISGs). They play an important role in the establishment of the cellular antiviral state, inhibition of viral infection and return to cellular homeostasis [3,9,14,16]. For example, the ectopic expression of heparinase (HPSE) can inhibit the attachment of multiple viruses [17,18]; interferon induced transmembrane proteins (IFITM) can impair the entry of multiple viruses and traffic viral particles to degradative lysosomes [19,20]; MX dynamin like GTPase proteins (MX) can effectively block early steps of multiple viral replication cycles [21]. Abnormality in the IFN-signalling cascade, for example, the absence of signal transducer and activator of transcription 1 (STAT1), will lead to the failure of activating ISGs, making the host cell highly susceptible to virus infections [22].

Figure 1. Illustration of signalling cascade triggered by different IFNs. In (A), type I IFN signals through IFNAR, Janus kinase 1(JAK1), tyrosine kinase 2 (TYK2), STAT, and IFN regulatory factor 9 (IRF9) to form IFN stimulated gene factor 3 complex (ISGF3), and binds to IFN stimulated response elements (ISRE) to induce the expression of type I ISGs. In (B), type II IFN signals through IFNGR, JAK1 and JAK2 to form IFN-γ activation factor (GAF) and binds to gamma-activated sequence promoter elements (GAS) to induce the expression of

type II ISGs. In (C), type III IFN signals through IFNLR1, IL-10R2, JAK1, TYK2, STAT, and IRF9 to form ISGF3, and then bind to ISRE to induce the expression of type III ISGs. Figure created using the BioRender (https://biorender.com/).

Most research on ISGs has focused on elucidating their role in antiviral activities or discovering new ISGs within or across species [3,9,14,19,23,24]. The identification of ISGs can be achieved via various approaches. Associating gene expression with suppression of viral infection is a good strategy to identify ISGs with obvious antiviral performance, exemplified by the influenza inhibitor, MX dynamin like GTPase 1 (MX1), and the human immunodeficiency virus 1 inhibitor, MX dynamin like GTPase 2 (MX2) [21]. CRISPR screening is a loss-of-function experimental approach to identify ISGs required for IFN-mediated inhibition to viruses. It enabled the discovery of tripartite motif containing 5 (TRIM5), MX2 and bone marrow stromal cell antigen 2 (BST2) [25]. Monitoring the ectopic expression of ISGs is another instrumental way to identify ISGs that are individually sufficient for viral suppression [26], for example, interferon stimulated exonuclease gene 20 (ISG20) and ISG15 ubiquitin like modifier (ISG15). Using RNA-sequencing [27] and fold change-based criterion to measure whether a target human gene is induced by IFN signalling is routinely used [24,28,29]. In most cases, a gene is defined as IFN stimulated (up-regulated) when its expression value is increased in the presence of IFNs (fold change > 2) [3,24,30].

There are several online databases to support IFN- or ISG-related research. For example, Interferome (http://www.interferome.org) provides an excellent resource by compiling *in vivo* and *in vitro* gene expression profiles in the context of IFN stimulation [24]. The Orthologous Clusters of Interferon-stimulated Genes (OCISG, http://isg.data.cvr.ac.uk) demonstrates an evolutionary comparative approach of genes differentially expressed in the type I IFN system for ten different species [3].

Experimental data in the Interferome database indicate that a human gene may show differential responses to different IFNs in different tissues or cells [24]. Despite some well-investigated ISGs, the majority of classified ISGs have limited expression following IFN stimulations [3,24]. This means that the difference between ISGs and those human genes not significantly up-regulated in the presence of IFNs (non-ISGs) may not be obvious especially when being assessed more generally. It should also be noted that, within non-ISGs, there are a group of genes down-regulated during IFN stimulations. We refer to them as interferon-repressed human genes (IRGs) and they constitute another major part of the IFN regulation system [3,31]. Collectively, the complex nature of the IFN-stimulated system results in knowledge that is far from comprehensive.

In this study, we try to associate the inherent properties of human genes with their expression following IFN-α stimulation. We show that it is feasible to make ISG predictions on human genes with a model only compiled from the knowledge of IFN-α responses in the human fibroblast cells. To achieve this, we first constructed a refined high-confidence dataset consisting of 620 ISGs and 874 non-ISGs by checking the genes across multiple databases including OCISG [3], Interferome [24], and Reference Sequence (RefSeq) [32]. The analyses were conducted primarily on our refined data using genome- and proteome-based features that were likely to influence the expression of human genes in the presence of IFN-α (**Figure 2**). Based on the calculated features, we designed a machine learning framework with an optimised feature selection strategy for the prediction of putative ISGs in different IFN systems. Finally, we also developed an online web server and Docker application to implement our machine learning method.

Figure 2. Diagrammatic representation of the project pipeline. Human genes used in analyses and machine learning modelling are classified based on their clinical representations

following IFN-α treatment in human fibroblast cells. ISGs (pink block) and non-ISGs (green block) in other IFN systems are only used for testing. The figure is created using images from Wikimedia Commons, https://commons.wikimedia.org.

Results

Evolutionary characteristics of ISGs

In this study, we constructed the dataset S2 from 10836 well-annotated human genes (dataset S1). It consists of 620 ISGs and 874 non-ISGs with high confidence based on their records in both the OCISG [3] and Interferome [24]. The compiled set of 10836 human genes were used as the background set and were evolutionarily unrelated to each other as they were retrieved from the OCISG [3] that compiled clusters of orthologous genes based on whole-genome alignments. Detailed information about our compiled datasets is provided in **Table 5** and **Supplementary Data S1**.

Here, we explored features relating to alternative splicing [33], duplication [34] and mutation [35]. We found that more highly upregulated human genes tended to have less open reading frames (ORFs) (Pearson's correlation coefficient (PCC) = -0.287, **Figure 3A**), transcripts (PCC = -0.407, **Figure 3B**), and protein-coding exons (PCC = -0.441, **Figure 3C**). These results illustrate that alternative splicing may be linked to IFN-α up-regulation. Particularly, the data points of IRGs are generally placed below those of non-ISGs, suggesting these three features (number of ORFs, number of transcripts and the usage of protein-coding exons) are all differentially represented in some IRGs compared to the remaining non-ISGs. This distribution also indicates that some IRGs have similar feature properties to ISGs, especially to those highly up-regulated in the presence of IFN-α (right part of the scatter plots in **Figure 3A, 3B & 3C**).

Figure 3. The average representation of alternative splicing **features associated with IFN-α stimulations in experiments.** (A) The numbers of ORFs and (B) transcripts are used as measurements of the diversity of alternative splicing process. (C) The counts of exons used for coding is used as a measurement of the complexity of alternative splicing process. These three plots are drawn based on the expression data of 8619 human genes with valid fold change in the IFN-α experiments (**Supplementary Data S1**). The 0.1-length sliding-window is adopted to divide the data into 126 bins with different Log_2(Fold Change). Vertical dashed lines x=-0.871 and x=0.686 are used to divide the plot into three regions. Data points in the left and right regions are produced by IRG and ISGs, respectively. Data points in the middle region come from ISGs or non-ISGs (including IRGs). 2217 human genes are not shown in these figures as they had insufficient read coverage to determine a fold change in the experiments (**Table 5**). Points in the scatter plot are located based on the average feature representation of genes with similar expression performance in experiments.

To determine whether the ISGs tend to originate from duplication events, we counted the number of within human paralogs of each gene (**Figure 4A**). We found that there were around 22% of singletons in our main dataset, whilst ISGs had 15% and non-ISGs had 26%. The result of a Mann-Whitney U test [36] indicated that the number of human paralogs was significantly under-represented in the ISGs compared to the background human genes (M_1 = 10.5, M_2 = 11.5, p = 8.8E-03). We hypothesize that such a difference is mainly caused by the imbalanced distribution of singletons in the ISGs and non-ISGs as it becomes smaller when singletons are excluded from the test (M_1 = 12.4, M_2 = 14.6, $p > 0.05$). Next, we used the number of non-synonymous substitutions per non-synonymous site (dN) and synonymous substitutions per synonymous site (dS) within human paralogues as a measurement of

differences in mutational signatures between different classes [37]. As shown in **Figure 4B**, non-synonymous substitutions are more frequently observed in the ISGs than in the background human genes (M_1 = 0.62, M_2 = 0.55, p = 4.0E-03). On the other hand, the ISGs also have a higher frequency of synonymous substitutions than the background human genes (M_1 = 37.7, M_2 = 34.6, p = 1.1E-02) (**Figure 4C**) but the difference is not as obvious as for non-synonymous substitutions. In **Figure 4D**, the distribution of dN/dS ratios within human paralogues indicates that most human genes are constrained by natural selection but the ISGs, in general, tend to be less conserved (M_1 = 0.036, M_2 = 0.045, p = 8.3E-03). When eliminating the influence of duplication events, the ISGs are still less conserved than the non-ISGs but the difference in the dN/dS ratio is not significant (M_1 = 0.053, M_2 = 0.031, p > 0.05).

Figure 4. Differences in the evolutionary constraints of human genes. (A) Paralogues within *Homo sapiens*. (B) Non-synonymous substitutions within human paralogues. (C) Synonymous substitutions within human paralogues. (D) dN/dS ratios within human paralogues. Here, the ISGs and non-ISGs are taken from dataset S2 while the background human genes are from dataset S1 (**Table 5**). Mann-Whitney U tests are applied for the hypothesis testing between the feature distribution of different classes. Boxes in the plot represent the major distribution of values (from the first to the third quartile); outliers are added for values higher than two-fold of the third quartile; cross symbol marks the position of the average value including the outliers; upper and lower whiskers show the maximum and minimum values excluding the outliers.

Differences in the coding region of the canonical transcripts

Compared to general profile features (e.g., number of ORFs), the sequences themselves provide more direct mapping to the protein function and structure [38]. Here, we encoded 344 discrete

features and 7026 categorical features from complementary DNA (cDNA) of the canonical transcript to explore features specific to ISGs. We divided the discrete features into four categories and compared their representations among three different groups of human genes including recompiled ISGs from dataset S2, recompiled non-ISGs from dataset S2, and the background human genes from dataset S1 (**Figure 5**).

Firstly, guanine and cytosine were both more depleted in ISGs than non-ISGs, leading to an under-representation of GC-content in the ISGs (Mann-Whitney U test: M_1 = 52%, M_2 = 55%, p = 2.3E-11). This attribute was antithetical to the GC-biased gene conversion (gBGC), making ISGs less stable with weak evolutionary conservation (**Figure 4**) [39]. Additionally, the under-representation of GC-content also influenced the representation of other dinucleotide features. Among all dinucleotide depletions in ISGs, CpG depletion was ranked the first followed by GpG and GpC depletions (p = 2.9E-14, 4.9E-13 and 1.2E-10, respectively). In turn, adenine and thymine-related dinucleotide compositions, exemplified by ApT and TpA were more enriched in ISGs than non-ISGs (p = 8.0E-10 and 8.5E-10, respectively).

We compared the usage of 64 different codons in the third category as their frequencies influence transcription efficiency [40]. Differences between the ISGs and background human genes were observed in codons for 11 amino acids including leucine (L), isoleucine (I), valine (V), serine (S), threonine (T), alanine (A), glutamine (Q), lysine (K), glutamic acid (E), arginine (R), and glycine (G). The most significant difference was observed in the usage of codon ‘AGA’. Among all arginine-targeted alternative codons, codon ‘AGA’ was usually favoured, and its usage reached an estimated 25% in the ISGs but reduced to 22% in the background human genes (p = 1.4E-05). It was even significantly lower in the non-ISGs, at 18% (p = 1.9E-13). On the other hand, compared to the background human genes, the codon ‘CAG’ coding for amino acid ‘Q’ was the most under-represented in the ISGs. It was less favoured by the ISGs than non-ISGs (M_1 = 72%, M_2 = 78%, p = 7.3E-13) although it dominated in coding

patterns. As for the three stop codons, comparing with the background human genes, the usage of the ochre stop codon ('TAA') was over-represented in the ISGs (M_1 = 28%, M_2 = 33%, p = 9.7E-03). In this category of codon usage, the features with different frequencies between the ISGs and background human genes became more discriminating when comparing the ISGs with non-ISGs. Significant differences in codon usages between the ISGs and non-ISGs were widely observed except for methionine (M) and tryptophan (W). Hence, despite the limited differences of codon usages between the ISGs and background human genes, these features were useful for discriminating the ISGs from non-ISGs.

In the last category, we calculated the occurrence frequency of 256 nucleotide 4-mers to add some positional resolution for finding and comparing interesting organisational structures [41]. Among the 256 4-mers, 46 of them were differentially represented between the ISGs and background human genes (**Supplementary Data S2**). Most of these 4-mers were over-represented by the ISGs except two with the pattern 'TAAA' and 'CGCG'. Interestingly, the feature of 'TAAA' composition became a positive factor when comparing ISGs and non-ISGs (M_1 = 4.1%, M_2 = 3.7%, p = 4.1E-06), suggesting it might be a good feature to discern potential or incorrectly labelled ISGs. We found six nucleotide 4-mers: 'ACCC', 'AGTC', 'AGTG', 'TGCT', 'GACC', and 'GTGC' were over-represented in the ISGs when compared to the background human genes. However, they were not differentially represented when comparing the ISGs with non-ISGs. These six features might be inherently biased for some reasons and were not powerful enough to contribute to distinguishing the ISGs from non-ISGs. In addition to the aforementioned 40 features (except 4-mer 'ACCC', 'AGTC', 'AGTG', 'TGCT', 'GACC', and 'GTGC') that were differentially represented in ISGs compared to background human genes, we found a further 39 features nucleotide 4-mers differentially represented between ISGs and non-ISGs (**Supplementary Data S2**).

To check the effect of these aforementioned 343 features on the level of stimulation in the IFN-α system (Log_2(Fold Change) > 0), we calculated the PCC for the normalised features (**Equation 2**) and found 106 features were positively related to the increase of fold change, and 34 features were suppressed when human gene were more up-regulated after IFN-α treatments (Student t-test: $p < 0.05$) (**Supplementary Data S3**). ApA composition showed the most obvious positive correlation with stimulation level (PCC = 0.464, p = 8.8E-06) while negative association between the representation of 4-mer 'CGCG' and IFN-α-induced up-regulation was the most significant (PCC = -0.593, p = 3.2E-09). Human genes with higher up-regulation in the presence of IFN-α contained more codons 'CAA', rather than 'CAG' for coding amino acid 'Q'. The depletion of GC-content, especially cytosine content, promotes the suppression of many nucleotide compositions in the cDNA, e.g. CpG composition.

Figure 5. Differences in the representation of discrete features encoded from coding regions (canonical). Mann-Whitney U tests are applied for hypothesis testing on the whole comparing data without sampling and the results are provided in the **Supplementary Data S2**. Here, the ISGs and non-ISGs are taken from dataset S2 (No. = 620 and 874) while the background human genes are from dataset S1 (No. = 10836) (**Table 5**).

To find conserved sequence patterns relating to gene regulations [42], we checked the existence of 2940, 44100 and 661500 short linear nucleotide patterns (SLNPs) consisting of three to five consecutive nucleobases in the group of the ISGs and non-ISGs. By using a positive 5% difference in the occurrence frequency as cut-off threshold, we found 7884 SLNPs with a maximum difference in representation around 15%. After using Pearson's chi-squared tests and Benjamini-Hochberg correction to avoid type I error in multiple hypotheses [43], 7025 SLNPs remained with an adjusted p-value lower than 0.01 (**Supplementary Data S4**),

hereon referred to as “flagged” SLNPs. The differentially represented 7025 SLNPs were ranked according to the adjusted p-value. As shown in **Figure 6A**, dinucleotide ‘TpA’ dominates in the top 10, top 100, top 1000, and all differentially represented SLNPs even if TpA representation is suppressed in the cDNA of genes’ canonical transcripts compared to other dinucleotides. Dinucleotide ‘ApT’ and ‘ApA’ are also frequently observed in the flagged SLNPs but their occurrences do not show significant difference in the top 100 SLNPs (Pearson's chi-squared test: $p > 0.05$). GC-related dinucleotides, e.g., ‘CpC’, ‘GpC’ and ‘GpG’ are rarely observed in the flagged SLNPs especially in the top 10 or top 100. In view of this, we hypothesize that the differential representation of nucleotide compositions influences and reflects on the pattern of SLNPs in the ISGs. By checking the co-occurrence status of the flagged SLNPs, we found that these sequence patterns had a cumulative effect in distinguishing the ISGs from non-ISGs especially when the number of cooccurring SLNPs reached around 5320 (Pearson's chi-squared test: $p = 7.9E-13$, **Figure 6B**). There were eight (~1.3%) ISGs in the dataset S2 containing all the flagged 7025 SLNPs. Their up-regulation after IFN-α treatment were generally low with a fold change fluctuating around 2.2. However, some of these eight genes such as desmoplakin (DSP) were clearly highly up-regulated in endothelial cells isolated from human umbilical cord veins after not only IFN-α treatments (fold change = 11.1) but also IFN-β treatments (fold change = 13.7). We also found some non-ISGs (e.g., hemicentin 1 (HMCN1)) and human genes with limited expression in the IFN-α experiments (ELGs) (e.g. tudor domain containing 6 (TDRD6)) containing the flagged SLNPs, but their frequencies were lower than that in the ISGs. Although there is an obvious imbalance between the number of the ISGs and non-ISGs in the human genome [9-11], the curve for the background human genes in **Figure 6B** is still closer to that for the ISGs rather than that for the non-ISGs. This suggests that some genetic patterns are widely represented in the coding region of human genes, making them potentially up-regulated in the IFN-α system.

Figure 6. SLNPs in the coding regions (canonical). (A) Influence of dinucleotide compositions on the flagged SLNPs. (B) The co-occurrence status of SLNPs in different human genes. Ranks in (A) are generated based on the adjust p value given by Pearson's chi-squared tests after Benjamini-Hochberg correction procedure. Detailed results of the hypothesis tests are provided in **Supplementary Data S4**. Here, the ISGs and non-ISGs are taken from dataset S2 while the background human genes are from dataset S1 (**Table 5**).

Differences in the protein amino acid sequence

We used the amino acid sequences generated by the canonical transcript to extract features at the proteomic level. In addition to the basic composition of 20 standard amino acids, we considered 17 additional features related to physicochemical (e.g., hydropathy and polarity) or geometric properties (e.g., volume) [44,45]. We found several amino acids that were either enriched or depleted in the ISG products compared to the background human proteins, which were produced by genes in dataset S1 (**Figure 7**). The differences were even more marked between protein products of the ISGs and non-ISGs, highlighting some differences that were not observed when comparing the ISG products to the background human proteins (e.g., isoleucine composition). The differences observed in the amino acid compositions were at least in part associated with the patterns previously observed in features encoded from genetic coding regions. For example, asparagine (N) showed significant over-representation in the ISG products compared to the non-ISG products or background human proteins (Mann-Whitney U test: p = 2.8E-12 and 1.2E-03, respectively). This was expected as there are only two codons, i.e., 'AAT' and 'AAC' coding for amino acid 'N', and dinucleotide 'ApA' showed a remarkable enrichment in the coding region of ISGs. A similar explanation could be given for the relationship between the deficiency of GpG content and amino acid 'G'. The translation of

amino acid ‘K’ was also influenced by ApA composition but was not significant due to the mild representation of dinucleotide ‘ApG’ in the genetic coding region. Additionally, as previously mentioned, the ISGs showed a significant depletion in the CpG content, and consequently, the amino acid ‘A’ and ‘R’ in the ISG products were significantly under-represented. Cysteine (C) was not frequently observed in human proteins but still showed a relatively significant enrichment in the ISG products (M_1 = 2.3%, M_2 = 2.5%, p = 1.8E-03).

When focusing on the composition of amino acids grouped by physicochemical or geometric properties, we found some features differentially represented between the ISG products and background human proteins. The result showed that hydroxyl (amino acid ‘S’ and ‘T’), amide (amino acid ‘N’ and ‘Q’), or sulfur amino acids (amino acid ‘C’ and ‘M’) were more abundant in the ISG products compared to the background human proteins (Mann-Whitney U test: p = 0.04, 1.0E-03 and 0.02, respectively). Small amino acids (amino acid ‘N’, ‘C’, ‘T’, aspartic acid (D) and proline (P), the volume ranges from 108.5 to 116.1 cubic angstroms) were more frequently observed in the ISG products than in background human proteins (M_1 = 22.1%, M_2 = 21.7%, p = 0.02). These differences became more marked when comparing the representation of these features between the ISG and non-ISG products. For example, features relating to chemical properties of the side chain (e.g., aliphatic), charge status and geometric volume showed differences between proteins produced by the ISGs and non-ISGs. Some features such as neutral amino acids that include amino acid ‘G’, ‘P’, ‘S’, ‘T’, histidine (H) and tyrosine (Y) were not differentially represented between the ISG and non-ISG products, but they indicated obvious association with the change of IFN-α-triggered stimulations (PCC = -0.556, p = 4.1E-08) (**Supplementary Data S3**).

Figure 7. Differences in the representation of discrete features encoded from protein sequences. Mann-Whitney U tests are applied for hypothesis testing on the whole data without

sampling and the results are provided in the **Supplementary Data S2**. Here, the ISGs and non-ISGs are taken from dataset S2 (No. = 620 and 874) while the background human genes are from dataset S1 (No. = 10836) (**Table 5**). Aliphatic group: amino acid ‘A’, ‘G’, ‘I’, ‘L’, ‘P’ and ‘V’; aromatic/huge group: amino acid ‘F’, ‘W’ and ‘Y’ (volume > 180 cubic angstroms); sulfur group: amino acid ‘C’ and ‘M’; hydroxyl group: amino acid ‘S’ and ‘T’; acidic/negative_charged group: amino acid ‘D’ and ‘E’; amide group: amino acid ‘N’ and ‘Q’; positive_charged group: amino acid ‘R’, ‘H’ and ‘K’; hydrophobic group: amino acid ‘A’, ‘C’, ‘I’, ‘L’, ‘M’, ‘F’, ‘V’, and ‘W’ that participates to the hydrophobic core of the structural domains [46]; neutral group: amino acid ‘G’, ‘H’, ‘P’, ‘S’, ‘T’ and ‘Y’; hydrophilic group: amino acid ‘R’, ‘N’, ‘D’, ‘Q’, ‘E’ and ‘K’; Tiny group: amino acid ‘G’, ‘A’ and ‘S’ (volume < 90 cubic angstroms); small group: amino acid ‘N’, ‘D’, ‘C’, ‘P’ and ‘T’ (volume ranged from 109 to 116 cubic angstroms); medium group: amino acid ‘Q’, ‘E’, ‘H’ and ‘V’ (volume ranged within 138 to 153 cubic angstroms); large group: amino acid ‘R’, ‘I’, ‘L’, ‘K’ and ‘M’ (volume ranged within 163 to 173 cubic angstroms); uncharged group: the remaining 15 amino acids except electrically charged ones; polar group: amino acid ‘R’, ‘H’, ‘K’, ‘D’, ‘E’, ‘N’, ‘Q’, ‘S’, ‘T’ and ‘Y’; nonpolar group: the remaining 10 amino acids except polar ones.

Next, we searched the sequence of the ISG products against that of the non-ISG products to find conserved short linear amino acid patterns (SLAAPs), which might be constrained by strong purifying selection [47]. As opposed to the analysis on the genetic sequence, we only obtained 19 enriched sequence patterns with a Pearson's chi-squared p value ranging from 1.5E-04 to 0.02 (**Table 1**), hereon referred to as flagged SLAAPs. They were greatly influenced by four polar amino acids: ‘K’, ‘N’, ‘E’ and ‘S’, and one nonpolar amino acid: ‘L’. Some of these flagged SLAAPs, for example, SLAAP ‘NVT’ and ‘S-N-E’, were clearly over-represented in the ISG products compared to the background human proteins and

could be used as features to differentiate the ISGs from background human genes. The third column in **Table 1** indicates a number of patterns that are lacking in the non-ISG products and hence may be the reason for the lack of up-regulation in the presence of IFN-α. Particularly, we noticed that SLAAP 'KEN' was a destruction motif that could be recognised or targeted by anaphase promoting complex (APC) for polyubiquitination and proteasome-mediated degradation [48,49]. Results shown in **Figure 8A** illustrate that the co-occurrence of differentially represented SLAAPs (flagged) has a cumulative effect in distinguishing the ISGs from non-ISGs. This cumulative effect can even be achieved with only two random SLAAPs (Pearson's chi-squared test: p = 4.6E-10). The bias in the co-occurring SLAAPs (flagged) in the background human proteins towards a pattern similar to the non-ISG products further proves the importance of these 19 SLAAPs. However, their co-occurrence is not associated with the level of IFN-triggered stimulations (PCC = 0.015, $p > 0.05$) (**Figure 8B**).

Regions that lacked stable structures under normal physiological conditions within proteins are termed intrinsically disordered regions (IDRs). They play an important role in cell signalling [50]. Compared with ordered regions, IDRs are usually more accessible and have multiple binding motifs, which can potentially bind to multiple partners [51]. According to the results calculated by IUPred [52], we found 6721, 10510, and 119071 IDRs (IUpred score no less than 0.5) in proteins produced by the ISGs, non-ISGs and background human genes respectively. We hypothesize that enriched SLAAPs widely detected in the IDRs may be important for human protein-protein interactions or potentially virus mimicry [53]. For instance, in the ISG products, about 40.8% of SLAAP 'SxNxT' were observed in the IDRs, 14.9% higher than that in non-ISG products (**Table 1**). This difference reflected the importance of SLAAP 'SxNxT' for target specificity of IFN-α-induced protein-protein interactions (PPIs) [9] even if it was not statistically significant. By contrast, the conditional frequency of SLAAP 'SxNxE' in the IDRs of the ISG and non-ISG products were almost the same, indicating that SLAAP

'SxNxE' might have an association with some inherent attributes of the ISGs but was less likely to be involved in the IFN-α-induced PPIs. SLAAP 'KEN' in the IDRs also showed some interesting differences: in the non-ISG products, 41.9% of SLAAP 'KEN' were observed in the IDRs, 14.6% higher than that in the ISG products, which provided an effective approach to distinguish the ISGs from non-ISGs. When SLAAP 'KEN' is discovered in the ordered globular region of a protein sequence, statistically, the protein is more likely to be produced by an ISG, but this assumption is reversed if the SLAAP is located in an IDR (Pearson's chi-squared tests: $p = 0.03$). Despite the relatively low conditional frequency of SLAAP 'KEN' in the IDRs of the ISG products, these SLAAPs in the IDR are more likely to be functionally active than those falling within ordered globular regions [54].

Table 1. Representation of SLAAPs in protein sequences and their IDRs.

SLAAP[a]	Frequency in ISG/non-ISG products[b]	Bias based on the frequency in human proteins	P value[c]	Conditional frequency in the IDRs of ISG/non-ISG products/background human proteins[c,d]	P value[e]
SxNxE	15.2%/8.8%	+47.6%/-14.2%	1.5E-04	39.4%/40.3%/33.4%	0.90
ENE	15.0%/8.8%	+20.9%/-29.0%	2.1E-04	37.6%/42.9%/40.9%	0.49
SxNxT	11.5%/6.2%	+21.9%/-34.2%	2.9E-04	40.8%/25.9%/27.3%	0.08
SVI	15.2%/9.2%	+37.6%/-16.9%	3.6E-04	18.1%/11.3%/15.2%	0.21
LxNL	23.7%/16.4%	+13.2%/-21.9%	4.0E-04	10.2%/11.9%/9.4%	0.65
LxKL	30.8%/22.8%	+18.0%/-12.8%	4.9E-04	12.6%/10.1%/8.7%	0.43
NVT	13.7%/8.5%	+52.1%/-6.1%	1.2E-03	18.8%/21.6%/15.4%	0.66
ISS	20.5%/14.3%	+20.7%/-15.7%	1.7E-03	29.9%/25.6%/23.8%	0.44
LKxK	24.4%/17.7%	+24.5%/-9.3%	1.8E-03	14.6%/20.6%/20.0%	0.16
IKxE	14.2%/9.0%	+34.2%/-14.5%	1.8E-03	26.1%/16.5%/25.8%	0.13
EKxI	15.8%/10.4%	+31.0%/-13.7%	2.0E-03	15.3%/20.9%/16.0%	0.32
KxExS	16.9%/11.4%	+21.9%/-17.7%	2.4E-03	36.2%/36.0%/39.2%	0.98
LNS	17.7%/12.1%	+21.2%/-17.1%	2.4E-03	20.0%/25.5%/20.5%	0.34
KEN	16.0%/10.6%	+33.5%/-11.0%	2.4E-03	27.3%/41.9%/34.8%	0.03
LxNxL	22.6%/17.5%	+14.3%/-11.4%	1.5E-02	10.7%/11.8%/9.5%	0.78
KxExL	25.8%/20.5%	+25.7%/-0.3%	1.5E-02	18.8%/17.9%/18.7%	0.84
KLL	27.1%/21.9%	+9.9%/-11.4%	1.9E-02	11.3%/8.4%/9.9%	0.35
LKE	29.8%/24.5%	+18.2%/-3.0%	2.1E-02	19.5%/24.8%/20.1%	0.20
LKxL	33.2%/27.7%	+15.0%/-4.2%	2.1E-02	7.8%/12.4%/10.0%	0.11

a: 'x' in SLAAPs indicates one position occupied by a standard amino acid;

*b: here, the ISGs and non-ISGs are taken from dataset S2 while the background human genes use samples from dataset S1 (**Table 5**);*

c: p values in this column use Pearson's chi-squared tests to measure the difference of SLAAPs occurrences in the ISG and non-ISG products;

d: frequencies in this column are calculated based on a condition that corresponding SLAAPs are observed in the protein sequence;

e: p values in this column use Pearson's chi-squared tests to measure the difference of SLAAPs occurrences in the IDRs of the ISG and non-ISG products.

Figure 8. Representation of co-occurring SLAAPs (flagged) in our main dataset. (A) The co-occurrence status of SLAAPs in different classes. (B) Relationship between co-occurrence of the marked SLAAPs and Log_2(Fold Change) after IFN-α treatments. Here, the ISGs and non-ISGs are taken from dataset S2 while the background human genes are from dataset S1 (**Table 5**). Points in (B) are located based on the average feature representation of genes with similar expression performance in IFN-α experiments.

Differences in network profiles

We constructed a network with 332,698 experimentally verified interactions among 17603 human proteins (confidence score > 0.63) from the Human Integrated Protein-Protein Interaction rEference (HIPPIE) database [55] to investigate if the connectivity among human proteins have association with genes' expression in the IFN-α experiments. 10169 out of 10836 human proteins produced by genes in our background dataset S1 were included in the network. Nodes and edges of this network can be downloaded from our webserver at http://isgpre.cvr.gla.ac.uk/. Based on this network, we calculated eight features as defined in the methods including the average shortest path, closeness, betweenness, stress, degree, neighbourhood connectivity, clustering coefficient, and topological coefficient.

As illustrated in **Figure 9B/G**, ISG products tend to have higher values of betweenness and stress than background human proteins (Mann-Whitney U test: p = 0.01, and 0.03, respectively), which means they are more likely to locate at key paths connecting different nodes of the PPI network. Some ISG products with high values of betweenness and stress, e.g.,

tripartite motif containing 25 (TRIM25), can be considered as the shortcut or bottleneck of the network and play important roles in many PPIs including those related to the IFN-α-triggered immune activities [56,57]. However, such differential representation of betweenness does not mean ISG products are more likely to be or even be close to bottlenecks of the network compared to the background human proteins. Some examples shown in **Table 2** indicate that ISG products are less-connected by top-ranked bottlenecks and hubs of the network than non-ISG products or the background human proteins. This conclusion is not influenced by hub/bottleneck protein's performance in the IFN-α experiments. Comparing proteins produced by the ISGs and non-ISGs, we found the former tends to have lower values of clustering coefficient and neighbourhood connectivity (Mann-Whitney U test: p = 0.04 and 7.9E-03, **Figure 9D/F**). This discovery indicates that the ISG products and some of their interacting proteins are less likely to be targeted by lots of proteins. It also supports the finding that the ISG products are involved in many shortest paths for nodes but are away from hubs or bottlenecks in the network. To some extents, this location also increases the length of the average shortest paths through ISG products in the network (**Figure 9A**).

When investigating the association between IFN-α-induced gene stimulation and network attributes of gene products, we only found the feature of neighbourhood connectivity was under-represented as the level of differential expression in the presence of IFN increases (PCC = -0.392, p = 2.2E-04). This suggests that proteins produced by genes that are highly up-regulated in response to IFN-α are further away from hubs in the PPI networks.

Figure 9. Differences in network preferences. The included features are: (A) average shortest path (B) betweenness, (C) closeness, (D) clustering coefficient, (E) degree, (F) neighbourhood connectivity, (G) stress, and (H) topological coefficient. Mann-Whitney U tests are applied for hypothesis testing on the whole comparing data without sampling and the results were provided

in the **Supplementary Data S2**. Here, the ISGs and non-ISGs are taken from dataset S2 (No. = 620 and 874) while the background human genes use samples from dataset S1 (No. = 10836) (**Table 5**).

Table 2. Interaction profiles of human proteins connecting top hubs/bottlenecks of the HIPPIE network.

Human protein	TRIM25	ELAVL1	ESR2	NTRK1
Gene class	ISG	IRG	Not included in S1[a]	
Degree (hub rank)	2295 (2nd)	1787 (4th)	2500 (1st)	1976 (3rd)
Betweenness (bottleneck rank)	0.067 (1st)	0.048 (4th)	0.051 (3rd)	0.026 (5th)
Difference in interacting partners (ISG products versus non-ISG products)[b]	Depleted P = 0.01	P > 0.05	Depleted P = 1.1E-4	Depleted P = 5.5E-3
Difference in interacting partners (ISG products versus the background human proteins)[b]	P > 0.05	P > 0.05	Depleted P = 8.1E-3	Depleted P = 0.03

a: ESR2 and NTRK1 were not included in dataset S1 as their expression data were not compiled in OCISG;

b: differences here are measured via Pearson's chi-squared tests on human proteins interacting with the corresponding hub/bottleneck protein.

Features highly associated with the level of IFN stimulations

In this study, we encoded a total of 397 discrete and 7046 categorical features covering the aspects of evolutionary conservation, nucleotide composition, transcription, amino acid composition, and network profiles. In order to find out some key factors that may enhance or suppress the stimulation of human genes in the IFN-α system, we compared the representation of discrete features of human genes with different but positive Log_2(Fold Change). Two features on the co-occurrence of SLNPs and SLAAPs were not taken into consideration here as they were more subjective than the other discrete features and were greatly influenced by the number of sequence patterns. Upon the calculation of PCC and the result of hypothesis tests, we found 168 features highly associated with the level of IFN-α-triggered stimulations (Student t-tests: $p < 0.05$) (**Supplementary Data S3**). Among them, 118 features showed a positive correlation (**Figure 10**) while the remaining 50 features showed a negative correlation (**Figure 11**) with the change of up-regulation in IFN-α experiments. Among these 168 features,

the number of ORFs, alternative splicing results, and counts of exons used for coding were encoded from characteristics of the gene. Average dN/dS and average dS within human paralogues were encoded based on the sequence alignment results from Ensembl [58]. 140 and 22 features were encoded from the genetic sequence and proteomic sequence respectively. The last one, neighbourhood connectivity, was obtained from the network profile of a human interactome constructed based on experimentally verified data in the HIPPIE database [55].

In the positive group, the feature of 'large' amino acid compositions that includes the composition of five amino acids with geometric volume ranged from 163 to 173 cubic angstroms was ranked the first for having the highest PCC at 0.593 (Student t-test: p = 2.8E-09). This feature was not highlighted previously as it did not have a strong signal for discriminating the ISGs from non-ISGs (Mann-Whitney U test: $p > 0.05$). Similar phenomena were found on 87 features (64 positive correlations and 23 negative correlations) such as AG-content, ApG content and previously mentioned neutral amino acid composition. The strongest negative correlation between feature representation and IFN-α-triggered stimulations was found on the feature of 4-mer 'CGCG' (PCC = -0.593, p = 3.2E-09). This feature also showed a differential distribution between the ISGs and non-ISGs, thus provided useful information to distinguish the ISGs from non-ISGs. Similar phenomena were found on 81 features (54 positive correlations and 27 negative correlations) such as previously mentioned GC-content, CpG content and the usage of codon 'GCG' coding for amino acid 'A'.

Collectively, the biased effect on the basic composition of nucleotides influences the correlation between the representation of sequence-based features and IFN-α-triggered stimulations. Human genes that show over-representation in more features listed in **Figure 10** are expected to be more up-regulated after IFN-α treatments at least in the human fibroblast cells. Meanwhile, the under-representation of features listed in **Figure 11** also contributes to the level of up-regulation in the IFN-α experiments.

Figure 10. 118 features positively associated with higher up-regulation after IFN-α treatments. Features here are screened based on the PCC and results of Student t-tests ($p < 0.05$). Features with higher PCC indicate stronger positive correlation. Detailed results about PCC and hypothesis tests are provided in **Supplementary Data S3**.

Figure 11. 50 features negatively associated with higher up-regulation after IFN-α treatments. Features here are screened based on the PCC and results of Student t-tests ($p < 0.05$). Features with lower PCC indicate stronger negative correlation. Detailed results about PCC and hypothesis tests are provided in **Supplementary Data S3**.

Difference in feature representation of interferon-repressed genes and genes with low levels of expression

We grouped human genes into two classes based on their response to the IFN-α in the human fibroblast cells. Genes significantly up-regulated in IFN-α experiments were included in the ISG class, while those that did not were put into the non-ISG class. However, there is also another group of human genes down-regulated in the presence of IFN-α, i.e., the IRGs. They were labelled as the non-ISGs, but contain unique patterns that constitute an important aspect of the IFN response [3]. Some of these IRGs were not up-regulated in any known type I IFN systems, thus have been placed in a refined non-ISG class for analyses and predictions. Additionally, there are a number of genes that have insufficient levels of expression in the experiments to determine a fold change, i.e., ELGs. Here, we used the previously defined features to compare the ISGs from dataset S2 with the IRGs and ELGs divided from the background dataset S1 (**Table 5**).

As shown in **Figure 12,** the IRGs are differentially represented to a lower extent in the majority of nucleotide 4-mer compositions than the ISGs, indicating the deficiency of some nucleotide sequence patterns in the coding region of IRGs. Note that, many nucleotide 4-mer composition features are more suppressed in the ISGs than non-ISGs although the differences are small. The biased representation of these features in the IRGs suggests that the IRGs have characteristics similar to the ISGs rather than non-ISGs. Additionally, there are a very limited number of features relating to evolutionary conservation, nucleotide compositions or codon usages showing obvious differences between the ISGs and IRGs, but many of them are differentially represented when comparing the ISGs with non-ISGs. Therefore, involving the IRGs in the class of the non-ISGs will increase the risk for machine learning models to produce more false positives. However, there are some informative features differentiating the IRGs from ISGs. For example, compared to the ISGs, the IRGs are more enriched in CpGs (Mann-Whitney U test: p = 5.6E-03), which is also mentioned in [59]. The IRGs tend to have higher closeness centrality and neighbourhood connectivity than the ISGs (Mann-Whitney U test: p = 0.04 and 6.4E-06 respectively), suggesting that the IRGs are closer to the centre of the human PPI network and connected to key proteins with many interaction partners. Differences in some amino acid composition features between the ISGs and IRGs can also be observed in **Figure 12**. Therefore, good predictability is still expected when using features extracted from proteins sequences.

Figure 12 also illustrates 161 features showing significant differences (Mann-Whitney U tests: $p < 0.05$) in the representation of the ISGs and ELGs. An estimated 82% of these features were also differentially represented between the ISGs and non-ISGs. 79% of these significant features displayed similar over-representation or under-representation in two comparisons, i.e., ISGs versus ELGs and ISGs versus non-ISGs. These ratios indicate that the majority of the ELGs are less likely to be ISGs based on their feature profile as well as their

low expression levels in cells induced with IFN-α. Network analyses showed that the ELG products tended to have lower values of all calculated network features than ISG products with the exception of topological coefficient. This means that the ELG products are less connected by other human proteins in the human PPI network. Particularly, their abnormal representation on the feature of average shortest paths indicating that some ELGs (e.g. vascular cell adhesion molecule 1 (VCAM1) and ubiquitin D (UBD)) may still have high connectivity in the human PPI network.

Figure 12. Differential expressions of discrete features between different genes and their coded proteins. Mann-Whitney U tests are applied for hypothesis testing on the whole comparing data without sampling and the results were provided in the **Supplementary Data S2**. Here, the ISGs and non-ISGs are taken from dataset S2 (No. = 620 and 874); the IRGs and ELGs are taken from dataset S4 (No. = 1006) and dataset S8 (No. = 2217); the background human genes are from dataset S1 (No. = 10836) (**Table 5**).

Implementation with machine learning framework

In this study, we encoded 397 discrete and 7046 categorical features for the analyses. As an excess of features will greatly increase the dimension of feature spaces and complicate the classification task for the classifier, we limited the number of SLNPs to the top 100 based on the adjusted p-value and we expected these to be sufficient to provide a picture of short linear sequence patterns in the coding region of the canonical transcript. Accordingly, features measuring the co-occurrence status of multiple SLNPs were recalculated based on the selected 100 SLNPs. As a result, we prepared 518 features (**Supplementary Data S5**) for our machine learning framework. To reduce the impact of noisy data on classifications, we only used the refined ISGs and non-ISGs from dataset S2 for training and modelling.

Table 3 firstly shows the comparisons of prediction performance among different machine learning methods. The threshold is determined by maximising the value of MCC. As the random forest (RF) classifier was built based on randomly selected samples and features [60], we repeated its modelling procedure ten times. These initial comparisons showed that the support vector machine (SVM) [61] is superior to k-nearest neighbors (KNN) and RF [60]. The poor prediction performance of the best base classifier (SVM, AUC = 0.6509) indicates that there are a number of noisy features hidden in the set. As some genes respond to IFNs in a cell-specific manner [2], it is hard to produce predictions unless we detect key discriminating features, which are robust to the change of biological environment.

Here, we considered two iterative strategies for selecting 'good' features. The first one is the forward feature selection (FFS) [62] wherein features are added sequentially based on their individual performance. This strategy did not work well (**Table 3**) as the prediction performances were all poor when the feature were used individually (**Supplementary Data S5**). The second strategy is developed based on the backward feature elimination scheme but uses less iterations to achieve the end result, namely AUC-driven subtractive iteration algorithm (ASI) (**Figure 15**).

Pre-processing using the ASI algorithm showed that there were at least 28% of features disrupting the prediction model. The loss of some of the individual nucleotide 4-mer feature seemed not to influence the performance of the classifier at this stage, but the similarities between IRGs and ISGs (**Figure 12**) particularly in the 4-mer features was a cause for concern when the model was used to predict new data especially unknown IRGs.

When using the ASI algorithm, the number of disrupting features did not stabilise until the algorithm reached the 11-th iterations. The remaining 74 features constituted our optimum feature set for predicting the ISGs (**Table 4**). Among them, 14 and 9 features displayed positive and negative correlations with the level of up-regulation in IFN-α experiments ($p < 0.05$).

During the procedure, the AUC kept increasing steadily and reached 0.7479 at the end (**Table 3**). The Matthews correlation coefficient (MCC) also showed an overall improvement although it fluctuated slightly during the last few iterations. By degressively ranking the score calculated by the prediction model, we found 68.1% of the 496 genes (equal to the number of ISGs in the training dataset) were successfully predicted as the ISGs. **Figure 13B** illustrates the distribution of prediction scores generated by the ASI-optimised model for human genes with different expressions in IFN-α experiments. Human genes with higher up-regulation in IFN-α experiments tend to obtain higher prediction score from our optimised machine learning model (PCC = 0.243, p = 4.2E-10).

However, there were also some ISGs incorrectly predicted by our model even though they were highly up-regulated, for example, basic leucine zipper ATF-like transcription factor 2 (BATF2, prediction score = 0.34). The model produced 33 ISGs with a prediction score higher than 0.8 but this number for the non-ISGs reduced to six, including one IRG (tripartite motif containing 59 (TRIM59)). The highest prediction score within the non-ISGs was found on ubiquitin conjugating enzyme E2 R2 (UBE2R2, prediction score = 0.88). It contains many features similar to the ISGs but was not differentially expressed in the presence of IFN-α in the human fibroblast cells [3]. The lowest prediction score within ISGs was found on cap methyltransferase 1 (CMTR1, prediction score = 0.12) due to the weak signal from its features. For instance, CMTR1 protein does not contain any ISG-favoured SLAAPs listed in **Table 1**. The influence of the IRGs on the prediction was reflected in the training dataset but was not significant. Compared with human genes not differentially expressed in the IFN-α experiments (non-ISGs but not IRGs), there were slightly more IRGs unsuccessfully classified when using a threshold of 0.549 (Pearson's chi-squared tests: M_1 = 27%, M_2 = 24%, $p > 0.05$).

Table 3. Performance of different machine learning classifiers on the training dataset S2' via five-fold cross-validation.

Classifier	Method	Features	Threshold-dependent					Threshold-independent	
			Score range	Threshold[a]	Sensitivity	Specificity	MCC	SN_496[b]	AUC
Basic	KNN[c]	518	0.100~0.900	0.500~0.550	0.593	0.621	0.214	0.607±0.014	0.6305
	RF[d]	Random	0.080~0.900	0.380~0.579	0.590±0.168	0.617±0.183	0.219±0.019	0.600±0.007	0.6413±0.0082
	SVM	518	0.328~0.743	0.542	0.567	0.681	0.250	0.615	0.6509
Optimised	SVM+FFS	78[e]	0.170~0.836	0.561	0.518	0.760	0.287	0.621	0.6768
	SVM+ASI	74[e]	0.098~0.918	0.549	0.623	0.750	0.376	0.681	0.7479

a: this threshold is provided by maximising the value of MCC;

b: this sensitivity is measured among tested genes with the top 496 prediction probabilities;

c: k-value here is set as the square root of the size of the training samples in five-fold cross validation, i.e., k = 20 [63];

d: this random forest algorithm uses 50 random grown trees and the modelling and validation procedures are repeated for ten times;

e: these features constitute the best/optimum feature set for the current machine learning method.

Figure 13. The optimisation on the machine learning model with the ASI algorithm. (A) shows the change of the prediction models based on the one generated with all 518 features (noisy feature vector = 144, best MCC = 0.250, SN_496 = 0.615, and AUC = 0.6509). (B) shows the distribution of prediction scores generated by the ASI-optimised model for human genes with different expression levels in the IFN-α system. The ISGs and non-ISGs shown in (B) are randomly selected through an undersampling strategy [64] on dataset S2. The list of gene names can be found in **Supplementary Data S1**.

Table 4. The optimum 74 features contributing to predicting the ISGs.

Evolutionary features (2)		
Number of human paralogues, average dS within human paralogues[N].		
Codon usage features (10)		
Codon usage: CTA (L)[P]	Codon usage: ATT (I)	Codon usage: TAT (Y)
Codon usage: GCG (A)[N]	Codon usage: CAC (H)[N]	Codon usage: TGC (C)
Codon usage: CGT (R)	Codon usage: CGA (R)	Codon usage: CGG (R)[N]
Codon usage: AGA (R)[P]		
Genetic composition features (40)		

DNA AC content	Dinucleotide CpT composition	DNA 4-mer CGCG composition^{N}
DNA 4-mer AATC composition^{P}	DNA 4-mer TCGT composition	DNA 4-mer GATG composition^{P}
DNA 4-mer AACA composition	DNA 4-mer TGAG composition^{P}	DNA 4-mer GACC composition
DNA 4-mer ATAT composition	DNA 4-mer TGTA composition	DNA 4-mer GACG composition
DNA 4-mer ATGT composition^{P}	DNA 4-mer CACG composition	DNA 4-mer GAGT composition^{P}
DNA 4-mer ACAC composition	DNA 4-mer CTCC composition	DNA 4-mer GTAC composition
DNA 4-mer ACTA composition	DNA 4-mer CCAC composition	DNA 4-mer GTGT composition
DNA 4-mer ACTC composition	DNA 4-mer CCTA composition	DNA 4-mer GTGC composition
DNA 4-mer ACCG composition	DNA 4-mer CCTC composition^{P}	DNA 4-mer GTGG composition
DNA 4-mer TATG composition	DNA 4-mer CCGT composition	DNA 4-mer GCAA composition^{P}
DNA 4-mer TTCT composition	DNA 4-mer CGAG composition	DNA 4-mer GCTC composition
DNA 4-mer TTCG composition	DNA 4-mer CGTG composition	DNA 4-mer GCCT composition
DNA 4-mer TTGA composition	DNA 4-mer CGCA composition	DNA 4-mer GGGG composition
DNA 4-mer TCAT composition		
Proteomic composition features (9)		
Arginine composition, cysteine composition^{P}, methionine composition;		
Basic amino acid composition (R/H/K)^{P}	Sulfur amino acid composition (C&M)^{P}	
Hydroxyl amino acid composition (S&T)^{N}	Small amino acid composition (N/D/C/P/T)^{N}	
Large amino acid composition (R/I/L/K/M)^{P}		
Uncharged amino acid composition (A/N/C/Q/G/I/L/M/F/P/S/T/W/Y/V)^{N}		
Features about human interactome network (3)		
Average shortest paths^{P}, betweenness, neighborhood connectivity^{N}.		
Sequence pattern features (8)		
SLNP: ATA[AG][TG]	SLNP: TAT[AT]T	SLNP: T[AT]AAA
SLNP: [ATG]TGTA	SLAAP: SxNxE	SLAAP: ENE
SLAAP: SVI	Co-occurrence of SLAAPs (count)	

P: features are positively associated with the level of up-regulation in IFN-α experiments ($p < 0.05$);

N: features are negatively associated with the level of up-regulation in IFN-α experiments ($p < 0.05$).

Review of different testing datasets

In this study, we trained and optimised a SVM model from our training dataset S2', and prepared seven testing datasets (dataset S2''/S3/S4/S5/S6/S7/S8) to assess the generalisation capability of our model under different conditions (**Table 5**). The S2'' testing dataset was a subset of dataset S2. The prediction performance on this testing dataset was close to that in the training stage with an AUC of 0.7455 (**Figure 13A**). The best MCC value (0.345) was achieved when setting the judgement threshold to 0.438, which meant that the prediction model was sensitive to signals related to ISGs. In this case, it performed predictions with high sensitivity but inevitably produced many false positives, especially within IRGs.

In the S3 testing dataset, we used 695 ISGs with low confidence. The overall accuracy (equals to SN as there were no negatives) only reached 44.0% when using a judgement threshold of 0.549, about 0.18 lower than SN under the same threshold in the training dataset

S2' (**Table 3**). It is expected as some of their inherent attributes make them slightly up-regulated, silent or even repressed (e.g., become non-ISGs in other IFN systems) in response to some IFN-triggered signalling. On this testing dataset, our machine learning model produced 38 (5.5%) ISGs with a prediction score higher than 0.8. This number was also lower than that on the training dataset S2'. It further indicates the relatively low confidence for the ISGs included in dataset S3.

The S4 testing dataset was constructed to illustrate our hypothesis that there are some patterns shared among the ISGs and IRGs at least in the IFN-α system in the human fibroblast cells. On this testing dataset, the prediction accuracy (equals to SP as there were no positives) was 60.2% under the judgement threshold of 0.549, about 0.15 lower than the SP under the same threshold in the training dataset S2' (**Table 3**). Leucine rich repeat containing 2 (LRRC2), carbohydrate sulfotransferase 10 (CHST10) and eukaryotic translation elongation factor 1 epsilon 1 (EEF1E1) showed strong signals of being ISGs (probability score > 0.9). In total, there were 56 (5.6%) IRGs being incorrectly predicted as ISGs with prediction scores higher than 0.8. This high score was found in an estimated 8.1% of the ISGs but was only observed in 1.2% of human genes not differentially expressed in the IFN-α experiments (**Figure 13B**). These results indicate that there is a considerable number of IRGs incorrectly predicted as ISGs in the S4 testing dataset due to their close distance to the ISGs in the high-dimensional feature space. This may be the case for many other datasets including dataset S2'', S5, S6, S7, and S8. It also supports our hypothesis about the shared patterns from the machine learning aspect and is consistent with the results shown in **Figure 12**.

The next three testing datasets (S5, S6, and S7) were collected from the Interferome database [24] to test the applicability of the machine learning model across different IFN types. The ISGs in these testing datasets were all highly up-regulated (Log_2(Fold Change) > 1.0) in the corresponding IFN systems while all the non-ISGs were not up-regulated after

corresponding IFN treatments (Log_2(Fold Change) < 0). The results shown in **Figure 14** reveals that the ISGs triggered by type I or III IFN signalling can still be predicted by our machine learning model, but the performance is limited to some extent (AUC = 0.6677 and 0.6754 respectively). However, it is almost impossible to make normal predictions with the current feature space for human genes up-regulated by type II IFNs (AUC = 0.5532).

Figure 14. The performance of our optimised model on different datasets. (A) and (B) illustrate the AUC and best MCC. S2' is the training dataset used in this study. It randomly includes 496 ISGs and an equal number of non-ISGs from dataset S2 that contains ISGs/non-ISGs with high confidence (**Table 5**). Evaluation on this dataset in (A) is processed via five-fold cross validation. S2'' is the testing dataset constructed with the remaining human genes in dataset S2. S5, S6, and S7 are collected from the Interferome database [24], including human genes with different responses to the type I, II and III IFNs, respectively. The label and usage of these human genes are provided in **Supplementary Data S1**.

The S8 testing dataset consisted of 2217 human genes that were insufficiently expressed in IFN-α experiments in the human fibroblast cells [3]. The results showed that there were around 41.2% ELGs being predicted as the ISGs when using a judgement threshold of 0.549. This was approximately 0.21 lower than the SN under the same threshold in the training dataset S2' (**Table 3**). It suggests that there are more non-ISGs than ISGs in this dataset, which is consistent with the results shown in **Figure 12**. Particularly, we found ten ELGs with prediction scores higher than 0.9: CD48 molecule, CD53 molecule, lipocalin 2 (LCN2), uncoupling protein 1 (UCP1), coiled-coil domain containing 68 (CCDC68), potassium calcium-activated channel subfamily M regulatory beta subunit 2 (KCNMB2), potassium voltage-gated channel interacting protein 4 (KCNIP4), zinc finger HIT-type containing 3 (ZNHIT3), serpin family B

member 4 (SERPINB4), and fibrinogen silencer binding protein (FSBP). By retrieving data from the Genotype-Tissue Expression project [65], we found that the expression of these ELGs were generally limited with the exception of CD53 and ZNHIT3 (**Figure 15**). The expression data of CD53 were not included in the OCISG database [3] and were also limited in the Interferome database [24]. It only showed slight up-regulation after type I IFN treatments in blood, liver, and brain but there is currently no record of its expression level in the presence of IFN-α in the human fibroblast cells. ZNHIT3 is another well-expressed gene lacking information in the OCISG. In the Interferome database [24], we found that ZNHIT3 could be up-regulated after IFN treatments in some fibroblast cells on skin. As for the remaining eight ELGs, despite their limited expression in the human fibroblast cells, their features suggest that they are very likely to be IFN-α stimulated in a currently untested cell type.

Figure 15. Expression of the ELGs in different tissues. Expression data for ten ELGs are collected from the Genotype-Tissue Expression project (https://gtexportal.org/) [65]. The tissues in red are not included in the Interferome database [24]. White boxes in the heatmap indicate that there is no data available for genes in the corresponding tissues. The overall expression level of these ten ELGs are reflected via human perspective photo retrieved from Expression Atlas (https://www.ebi.ac.uk/gxa) [66].

Discussion

In this study, we investigated the characteristics that influence the expression of human genes in IFN-α experiments. We compared the ISGs and non-ISGs through multiple procedures to guarantee strong signals for the ISGs and to avoid cell-specific influences that resulted in the lack of the ISGs expression in certain cell types [2]. Even some highly up-regulated ISGs can

become down-regulated when the biological conditions change, exemplified by the performance of C-X-C motif chemokine ligand 10 (CXCL10) on liver biopsies after IFN-α treatment. This refinement is necessary as the representation of features between the ISGs and background human genes show that many non-ISGs especially IRGs have similar feature patterns to the ISGs (**Figure 12**).

Generally, the ISGs are less evolutionarily conserved with more human paralogues than the non-ISGs. They have specific nucleotide patterns exemplified by the depletion of GC-content and have a unique codon usage preference in coding proteins. There are a number of SLNPs widely observed in the cDNA of the ISGs which are relatively rare in the non-ISGs (**Supplementary Data S4**). Likewise, there are also many SLAAPs highlighted in the sequences of ISG products that are absent or rare in the non-ISG products (**Table 1**). In the human PPI network, the ISG products tend to have higher betweenness than the background human protein, indicating their more frequent interruption of the shortest path (geodesic distance) between different nodes. Abnormal expression or knockout of these proteins will increase the diameter of the network and may lead to some lethal consequences that are not tolerated in signalling pathways [67-69]. These ISG specific patterns may be the result of the evolution of the innate immune system in vertebrates and could be adaptations to the cellular environment induced by interferon following a pathogenic infection [70]. It is also possible that some of the particular SLNPs and SLAAPs may be functionally important as the cell changes from non-infected to infected. Experimental evidence will be necessary to investigate this.

Some inherent properties of the ISGs facilitate or elevate their expression after IFN-α treatments but may also be used by viruses to escape from IFN-α-mediated antiviral response [22]. For instance, the representation of dN showed a more significant difference than that of dS within human paralogues. We found that higher dN/dS ratio was positively correlated with

gene up-regulation following IFN-α treatments (**Figure 10**). It means the gene is less conserved with more non-synonymous or nonsense mutations, which can often be associated to inherited diseases and cancer [71]. It will also facilitate the virus to interfere with IFN-α signalling through the JAK-STAT pathway and inactivate downstream cellular factors involved in IFN-α signal transductions [22]. We found arginine was under-represented in the ISG products compared to the non-ISG products. As arginine is essential for the normal proliferation and maturation of human T cells [72], such depletion in the ISG products may leave a risk of inhibiting T- cell function and potentially increased susceptibility to infections [73]. Furthermore, the special pattern of the ISGs also promotes the representation of some features even if they are not well represented in nature, for example, the higher cysteine composition in the ISGs. We hypothesize that it may be helpful to activate T-cell to regulate protein synthesis, proliferation and secretion of immunoregulatory cytokines [74,75]. There are also some features (e.g. methionine composition) not differentially represented between the ISGs and non-ISGs but play important roles in IFN-α-mediated immune responses. For example, there is evidence for the methionine content playing a role in the biosynthesis of S-Adenosylmethionine (SAM), which can improve interferon signalling in cell culture [76,77].

As previously mentioned, there were similar patterns between the feature representation of the ISGs and IRGs, which led to the unclear boundary for the ISGs and non-ISGs in the feature space. We found significant differences on the representation of features on evolutionary conservation (**Figure 4**) between the ISGs and non-ISGs, but they became non-significant when comparing the ISGs with IRGs. Similar phenomena were observed on many features deciphered from the canonical transcript, e.g., dinucleotide composition and codon usage features. We suggest that the IRGs can be viewed as additional ISGs as they also regulate the activity of human genes in response to IFNs, only negatively. Furthermore, despite so many similarities between the ISGs and IRGs, the separate classification of these genes is still

possible. 4-mer compositions can be considered as the key features as most of them are differentially represented between ISGs and IRGs (**Figure 12**). Using proteomic features can also help to differentiate the ISGs from IRGs but is not as good as using 4-mer features.

In the machine learning framework, we developed the ASI algorithm to remove noisy features but kept features not influencing the prediction performance when being removed individually during iterations. Features might have synergistic effects thus the elimination of each feature left a different impact on the remaining ones even if these were individually useless for the improvement of the classifier. In this case, keeping as many useful features as possible seems to be a good option but will greatly increase the dimension of the feature space and increase the risk of overfitting [78]. By contrast, our ASI algorithm avoided such a risk and kept the synergistic effect of different features through iterations.

In the prediction task, we found some previously labelled non-ISGs with very high prediction scores, suggesting that they had many inherent properties enabling them to be stimulated after IFN-α treatments. Some of them, for example, UBE2R2 has been shown to be significantly up-regulated after IFN-α treatment [79]. The non-ISG label was assigned because the relevant expression data in the presence of IFN-α were not included in the OCISG [3] and Interferome databases [24]. We also found ten ELGs with very high prediction scores (> 0.9). Literature searches on these genes indicate that they are likely to be involved in the innate immune response [80,81]. Their responses may be limited to certain tissues or cell types for which there is limited expression data in the Interferome database [24]. For example, LCN2 has been shown to mediate an innate immune response to bacterial infections by sequestering iron [80] and is induced in the central nervous system of mice infected with West Nile virus encephalitis [82]. CD48 was shown to increase in levels in the context of human IFN-α/β/γ stimulation [81]. Interestingly, CD48 is also the target of immune evasion by viruses [83] and has been captured in the genome of cytomegalovirus and undergone duplication [84]. Evidence

for other ELGs is harder to assess, particularly those for which expression is absent in a range of tissues (e.g., UCP1 in **Figure 15**). UCP1 is a mitochondrial carrier protein expressed in brown adipose tissue (BAT) responsible for non-shivering thermogenesis [85]. It is possible that UCP1 is stimulated directly or indirectly by IFN-α in BAT, resulting in the defended elevation of body temperature in response to infection.

We developed the machine learning model based on experimental data from the human fibroblast cells stimulated by IFN-α. It can be generalised to type I or III IFN systems, presumably because activations of type I and III ISGs are both controlled by ISRE [9] and aim to regulate host immune response [10-12]. However, our model cannot be used for predictions in the type II IFN system (AUC = 0.5532, best MCC = 0.083, **Figure 14**). It may be caused by the different control element and the different role in human immune activities [14]. One feasible strategy is to reclassify the ISGs and non-ISGs for the type II IFN system. Using overlapping ISGs and non-ISGs in both type I and type II IFN system for modelling could also be promising.

In summary, our analyses highlight some key sequence-based features that are helpful to distinguish the ISGs from non-ISGs or IRGs. Our machine learning model is able to produce a list of putative ISGs to support IFN-related research. As knowledge of the ISG functions continue to be elucidated by experimentalists, the *in-silico* approach applied here can in future be extended to classify the different functions of ISGs. The ‘important’ features mentioned in this study may become a focus for investigating the interferon antagonists expressed by different viruses [86].

Methods

Dataset curation

In this study, we retrieved 2054 ISGs (up-regulated), 12379 non-ISGs (down-regulated or not differentially expressed), and 3944 unlabelled human genes (ELGs with less than one count per million reads mapping across the three biological replicates [87,88]) from the OCISG database (http://isg.data.cvr.ac.uk/) [3]. Gene clusters in the OCISG database were built through Ensembl Compara [89], which provided a thorough account of gene orthology based on whole genomes available in Ensembl [58]. Labels of these human genes were defined based on the fold change and a false discovery rate (FDR) following the IFN-α treatments in the human fibroblast cells. We searched the collected 18377 entries against the RefSeq database (https://www.ncbi.nlm.nih.gov/refseq/) [32] to decipher features based on appropriate transcripts (canonical) [90] coding for the main functional isoforms of these human genes. It produced 1315, 7304, and 2217 results for the ISGs, non-ISGs and ELGs, respectively. These 10836 human genes were well-annotated by multiple online databases and were used as the background dataset S1 in the analyses.

For the purpose of generating a set of human genes with high confidence of being up-regulated and non-up-regulated in response to the IFN-α, we searched the recompiled 8619 human genes (ISGs or non-ISGs) against Interferome (http://www.interferome.org/) [24]. We filtered out the ISGs without high up-regulation (Log_2(Fold Change) > 1.0) or with obvious down-regulation (Log_2(Fold Change) < -1.0) in the presence of type I IFNs. This procedure guaranteed a refined ISG dataset with strong levels of stimulation induced by any type I IFNs and reduced biases driven by the IRGs for the analyses and predictions. We filtered out the non-ISGs showing enhanced expression after type I IFN treatments (Log_2(Fold Change) > 0). The exclusion of these non-ISGs could effectively reduce the risk of involving false negatives

in analyses and producing false positives in predictions. As a result, the refined dataset S2 contains 620 ISGs and 874 non-ISGs with relatively high confidence.

The training procedure in the machine learning framework was conducted on the balanced dataset S2'. It consisted of 992 randomly selected ISGs and non-ISGs from dataset S2. The remaining human genes in S2 were used for independent testing. Additionally, we also constructed another six testing datasets for the purpose of review and assessment. Dataset S3 contained 695 ISGs with low confidence compared to those ISGs in dataset S2. Some of them could be non-ISGs or even IRGs in the type I IFN system. Dataset S4 contained 1006 IRGs from the human fibroblast cell experiments. Dataset S5, S6, and S7 were constructed based on records for experiments in type I, II, and III IFN systems from Interferome [24]. The criterion for an ISG in the latter three datasets was a high level of up-regulation (Log_2(Fold Change) > 1.0) while that for non-ISGs was no up-regulation after IFN treatments (Log_2(Fold Change) < 0). The last testing dataset S8 was derived from our background dataset S1, containing 2217 ELGs. A breakdown of the aforementioned eight datasets is shown in **Table 5**. Detailed information of the human genes used in this study is provided in **Supplementary Data S1**. The cDNA and protein sequences are accessible at http://isgpre.cvr.gla.ac.uk/.

Table 5. A breakdown of datasets used in this study.

Dataset	Brief description	IFN system	ISGs	Non-ISGs	ELGs	Usage
S1	Background human genes	IFN-α in fibroblast cells	1315	7304	2217	Analyses
S2	Dataset with high confidence	IFN-α in fibroblast cells	620	874	0	Analyses
S2'	Training subset of S2	IFN-α in fibroblast cells	496	496	0	Training
S2''	Testing subset of S2	IFN-α in fibroblast cells	124	378	0	Testing
S3	ISGs with low confidence in S1	IFN-α in fibroblast cells	695	0	0	Testing
S4	IRGs divided from S1	IFN-α in fibroblast cells	0	1006	0	Analyses/ testing
S5	ISGs from Interferome [24]	Type I IFNs in all cells	1259	872	0	Testing
S6	ISGs from Interferome [24]	Type II IFN in all cells	2229	755	0	Testing
S7	ISGs from Interferome [24]	Type III IFN in all cells	33	1683	0	Testing
S8	ELGs divided from S1	IFN-α in fibroblast cells	0	0	2217	Testing

Generation of discrete features

We encoded 397 discrete features from aspects of evolution, nucleotide composition, transcription, amino acid composition, and network preference. Original values of these features for our compiled 10836 human genes are accessible at http://isgpre.cvr.gla.ac.uk/.

From the perspective of evolution, we used the number of transcripts, open reading frames (ORFs) and count of exons used for coding to quantify the alternative splicing process. Genes with more transcripts and ORFs have higher alternative splicing diversity to produce proteins with similar or different biological functions [33,91,92]. Frequent use of protein-coding exons indicates more complex alternative splicing products [93]. Here, duplication and mutation features were measured by the number of within species paralogues and substitutions [34,35]. These data were collected from BioMart [58] to assess the selection on protein sequences and mutational processes affecting the human genome [94].

From the perspective of nucleotide composition, we calculated the percent of adenine, thymine, cytosine, guanine, and their four-category combinations in the coding region of the canonical transcript. The first category measured the proportion of two different nitrogenous bases out of the implied four bases, e.g., GC-content. The second category also focused on the combination of two nucleotides but added the impact of phosphodiester bonds along the 5' to 3' direction, e.g., CpG-content [95]. The third category calculated the occurrence frequency of 4-mers, e.g., 'CGCG' composition to involve some positional resolution [41]. The last category considered the co-occurrence of SLNPs. From the perspective of transcription, we calculated the usage of 61 coding codons and three stop codons in the coding region of the canonical transcripts. Codon usage biases are observed when there are multiple codons available for coding one specific amino acid. They can affect the dynamics of translation thus regulate the efficiency of translation and even the folding of the proteins [40,96].

From the perspective of amino acid composition, we calculated the percentage of 20 standard amino acids and their combinations based on their physicochemical properties [46]. Patterns in the amino acid level are considered to have a direct impact on the establishment of biological functions or to reflect the result of strong purifying selection [47]. Based on the chemical properties of the side chain, we grouped amino acids into seven classes including aliphatic, aromatic, sulfur, hydroxyl, acidic, amide, and basic amino acids. We also grouped amino acids based on geometric volume, hydropathy, charge status, and polarity, but found some overlaps among these features. For instance, amino acids with basic side chains are all positively charged. Aromatic amino acids all have large geometric volumes (volume > 180 cubic angstroms). Likewise, we also considered the co-occurrence of short linear sequence patterns at the protein level. These co-occurring SLAAPs may relate to potential mechanisms regulating the expression of the ISGs [97].

When trying to measure the network preference for the gene products, we constructed a human PPI network based on 332,698 experimentally verified interactions (confidence score > 0.63) from HIPPIE [55]. Nodes and edges of this network are provided at http://isgpre.cvr.gla.ac.uk/. Eight network-based features including the average shortest path, closeness, betweenness, stress, degree, neighbourhood connectivity, clustering coefficient, and topological coefficient were calculated from this network. Isolated nodes or proteins were not included in our network and were assigned zero value for all these eight features. The shortest path measures the average length of the shortest path between a focused node and others in the network. Closeness of a node is defined as the reciprocal of the length of the average shortest path. Proteins with a low value of the shortest paths or closeness are close to the centre of the network. Betweenness reflects the degree of control that one node exerted over the interactions of other nodes in the network [98]. Stress of a node measures the number of shortest paths passing through it. Proteins with a high value of betweenness or stress are close to the

bottleneck of the network. Degree of a node counts the number of edges linked to it while neighbourhood connectivity reflected the average degree of its neighbours. Proteins with high degree or neighbourhood connectivity are close to the hub of the network. They are considered to play an important role in the establishment of the stable structure of the human interactome [99]. Clustering and topological coefficient measure the possibility of a node to form clusters or topological structures with shared neighbours. The former coefficient can be used to identify the modular organisation of metabolic networks [100] while the latter one may be helpful to find out virus mimicry targets [53].

Generation of categorical features

In this study, categorical features were used to check the occurrence of short linear sequence patterns in the genome and proteome. SLNPs constructed in this study contained three to five random nucleotides, producing 708,540 alternative choices. SLNPs with no restrictions on their first or last position were not taken into consideration as their patterns could be expressed in a more concise way. A SLNP was picked out to encode a binary feature when its occurrence level in the coding region of the canonical ISG transcripts was significantly higher than that for the non-ISGs (Pearson's chi-squared test: $p < 0.05$). SLAAPs were constructed with three to four fixed amino acids separated by putative gaps. The gap could be occupied by at most one random amino acid, producing 1,312,000 alternative choices. Likewise, binary features were prepared for SLAAPs showing significant enrichment in the ISG products than in the non-ISG products (Pearson's chi-squared test: $P < 0.05$). Since there were lots of results rejecting the null-hypothesis, we adopted the Benjamini-Hochberg correction procedure to avoid type I error [43]. Additionally, we also encoded two features to check the co-occurrence or absence of multiple SLNPs and SLAAPs. This co-occurrence status might be a better

representation of functional sites composed of short stretches of adjacent nucleobases or amino acids surrounding SLNPs or SLAAPs [47].

Assessment of associations between feature representation and IFN-triggered stimulations

We obtained 8619 human genes with expression data from the OCISG database [3]. 4111 of them were annotated with a positive Log_2(Fold Change) ranging from 0 to 12.6, which meant they were up-regulated after IFN-α treatments in the human fibroblast cells. In order to measure the average level of feature representation (AREP) for genes with similar expression during IFN stimulations, we introduced a 0.1-length sliding-window to divide the data into 126 bins with different Log_2(Fold Change). Here, PCC was introduced to test the association between the representation of discrete features and IFN-α-triggered stimulation (Log_2(Fold Change) > 0). It can be formulated as:

$$PCC(f) = \frac{1}{n-1}\sum_{i=1}^{n}\left(\frac{LFC_i - M_0}{SD_0}\right) \times \left(\frac{AREP_i - M_f}{SD_f}\right) \quad \textbf{(1)}$$

where n is the number of divided parts that equals to 126 in this study; LFC_i and $AREP_i$ are the value of Log_2(Fold Change) and AREP in the i-th part; M_0 and SD_0 are the mean and standard deviation of Log_2(Fold Change), which is set as 6.4 and 3.7 respectively in this study; M_f and SD_f are the mean and standard deviation of 126 AREP that reflect the representation of the considered feature. To make fair comparisons among features with different scales, we normalised them based on the major value of their representations:

$$Norm(f) = \begin{cases} 1, f > UB(f) \\ \dfrac{f - LB(f)}{UB(f) - LB(f)}, LB(f) < f < UB(f) \\ 0, f < LB(f) \end{cases} \quad \textbf{(2)}$$

where $LB(f)$ and $UB(f)$ are the lower and upper bound representing the 5th and 95th percentile within representation values for the target feature. The representation of feature was

considered to have a stronger positive/negative association with IFN-α-triggered stimulations if the PCC calculated from the normalised features was closer to 1.0/-1.0 and the p value calculated by the Student t-test was lower than 0.05.

Machine learning and optimisation

We designed a machine learning framework for the prediction of ISGs. Firstly, all features were encoded and normalised based on their major representations (**Equation 2**). Then we used an under-sampling procedure [64] to generate a balanced dataset from dataset S2 for training and modelling. The SVM with radial basis function [61] was used as the basic classifier. It maps the normalised feature space to a higher dimension to generate a space plane to better classify the majority of positive and negative samples. In order to avoid overfitting [78] and made it easier for the SVM model to generate an appropriate classification plane that involved fewer false positives and false negatives, here, we propose a subtractive iteration algorithm driven by the change of AUC. This algorithm is developed based on the traditional backward feature elimination method [62] but uses fewer iterations to filter out noisy features (**Figure 16**). In each iteration, we traversed the features and removed those that did not improve the AUC of the prediction results. In the testing procedure, we encoded the optimum features for testing samples and placed them in the optimised feature space. Samples with longer distance to the optimised classification plane indicated a stronger signal of being the ISGs or non-ISGs. They were more likely to get higher prediction scores (close to 0 or 1) from the SVM model.

Figure 16. The pseudo-code of the AUC-driven subtractive iteration algorithm.

Performance evaluation

In this study, the prediction results were evaluated with three threshold-dependent criteria including sensitivity, specificity, and MCC [101] and two threshold-independent criteria: SN_n and AUC. SN and SP were used to assess the quality of the machine learning model in recognising ISGs and non-ISGs respectively while MCC provided a comprehensive evaluation for both positives and negatives. The number of 'n' in the SN_n criterion was determined based on the number of ISGs used for testing. It was used to measure the upper limit of the prediction model as well as to check the existence of important false positives close to the class of ISGs from the perspective of data expression. Finally, AUC was a widely used criterion to evaluate the prediction ability of a binary classifier system. The group of interest was almost unpredictable in a specific binary classifier system if the AUC of the classifier was close to 0.5.

Availability of source code and requirements

- Project name: ISGPRE
- Project home page: http://isgpre.cvr.gla.ac.uk/
- Operating system: Platform independent
- Programming language: Java
- Other requirements: Docker or JDK 8+
- Docker image: https://hub.docker.com/repository/docker/hchai01/isgpre
- Documentation and tutorials: https://github.com/HChai01/ISGPRE
- License: GNU GPL v3.0

Additionally, we have released all of our compiled data and calculated features at the project home page and GitHub repository. They can be reused to conduct research relating to IFN-α or type I/II/III IFNs.

Data Availability

The implemented web server and all reproduceable data are freely accessible at http://isgpre.cvr.gla.ac.uk/ and https://github.com/HChai01/ISGPRE.

Additional Files

Supplementary Data S1. Basic information and usage of our compiled 10836 human genes.

Supplementary Data S2. The result of Mann-Whitney U tests for discrete features.

Supplementary Data S3. Association between feature representations and IFN-α stimulations.

Supplementary Data S4. The result of Pearson's chi-squared tests for sequence motifs.

Supplementary Data S5. Features and their individual performance in machine learning.

Abbreviations

APC: anaphase promoting complex; AREP: average level of feature representation; ASI: AUC-driven subtractive iteration algorithm; AUC: area under the receiver operating characteristic curve; BAT: brown adipose tissue; BATF2: basic leucine zipper ATF-like transcription factor 2; BST2: bone marrow stromal cell antigen 2; CCDC68: coiled-coil domain containing 68; cDNA: complementary DNA; CHST10: carbohydrate sulfotransferase 10; CMTR1: cap methyltransferase 1; CXCL10: C-X-C motif chemokine ligand 10; dN: non-synonymous substitutions per non-synonymous site; dS: synonymous substitutions per synonymous site; DSP: desmoplakin; EEF1E1: eukaryotic translation elongation factor 1

epsilon 1; ELAVL1: embryonic lethal, abnormal vision like RNA binding protein 1; ELGs: human genes with limited expression in the IFN-α experiments; ESR2: estrogen receptor 2; FDR: false discovery rate; FFS: forward feature selection; FSBP: fibrinogen silencer binding protein; GAF: IFN-γ activation factor; GAS: gamma-activated sequence promoter elements; gBGC: GC-biased gene conversion; HIPPIE: Human Integrated Protein-Protein Interaction rEference; HMCN1: hemicentin 1; HPSE: ectopic expression of heparinase; IDRs: intrinsically disordered regions; IFITM: interferon induced transmembrane proteins; IFNAR: interferon-α receptor; IFNGR: IFN-γ receptor; IFNLR1: IFN-λ receptor 1; IFNs: interferons; IL-10R2: interleukin-10 receptor 2; IRF9: interferon regulatory factor 9; IRG: interferon repressed (down-regulated) human genes; ISG15: ISG15 ubiquitin like modifier; ISG20: interferon stimulated exonuclease gene 20; ISGF3: interferon stimulated gene factor 3 complex; ISGs: interferon stimulated (up-regulated) human genes; ISRE: interferon stimulated response elements; JAK1: Janus kinase 1; KCNIP4: potassium voltage-gated channel interacting protein 4; KCNMB2: potassium calcium-activated channel subfamily M regulatory beta subunit 2; KNN: k-nearest neighbors; LCN2: lipocalin 2; LRRC2: Leucine rich repeat containing 2; MCC: Matthews correlation coefficient; MX: MX dynamin like GTPase proteins; non-ISGs, human genes not significantly up-regulated by interferons; NTRK1: neurotrophic receptor tyrosine kinase 1; OCISG: Orthologous Clusters of Interferon-stimulated Genes; ORF: open reading frame; PCC: Pearson's correlation coefficient; PPI: protein-protein interaction; RefSeq: Reference Sequence; RF: random forest; SAM: S-Adenosylmethionine; SERPINB4: serpin family B member 4; SLAAP: short linear amino acid pattern; SLNP: short linear nucleotide pattern; SN: sensitivity; SP: specificity; STAT: signal transducer and activator of transcription; SVM: support vector machine; TDRD6: tudor domain containing 6; TRIM25: tripartite motif containing 25; TRIM5: tripartite motif containing 5; TRIM59: tripartite motif containing 59; TYK2: tyrosine kinase 2; UBD: ubiquitin D; UBE2R2: ubiquitin conjugating enzyme E2 R2;

UCP1: uncoupling protein 1; VCAM1: vascular cell adhesion molecule 1; ZNHIT3: zinc finger HIT-type containing 3.

Competing Interests

The authors have declared that no competing interests exist.

Funding

HC is supported by the China Scholarship Council (201706620069). JH, QG and DLR are supported by the Medical Research Council (MC_UU_1201412). The funders had no role in study design, data collection and analysis, decision to publish, or preparation of the manuscript.

Authors' Contributions

Conceptualization: all authors; data curation: H. C.; formal analysis: H. C.; funding acquisition: D. L. R.; investigation: H. C.; methodology: H. C.; project administration: D. L. R., J. H.; resources: Q. G., J. H., D. L. R.; web server: H. C.; software: H. C.; supervision: Q. G., J. H., D. L. R.; validation: all authors; visualization: H. C.; writing original draft: H. C.; writing review & editing: all authors.

Acknowledgments

The authors wish to thank Drs Andrew Davison, Suzannah Rihn and Sam Wilson for helpful discussions and recommendations, and Scott Arkison for help setting up the website.

References

1. Rönnblom L. The type I interferon system in the etiopathogenesis of autoimmune diseases. Ups J Med Sci. 2011;116(4):227-37.
2. Mostafavi S, Yoshida H, Moodley D, LeBoité H, Rothamel K, Raj T, et al. Parsing the interferon transcriptional network and its disease associations. Cell. 2016;164(3):564-78.
3. Shaw AE, Hughes J, Gu Q, Behdenna A, Singer JB, Dennis T, et al. Fundamental properties of the mammalian innate immune system revealed by multispecies comparison of type I interferon responses. PLoS Biol. 2017;15(12):e2004086.
4. Shalhoub S. Interferon beta-1b for COVID-19. The Lancet. 2020;395(10238):1670-1.
5. Harris BD, Schreiter J, Chevrier M, Jordan JL and Walter MR. Human interferon-ϵ and interferon-κ exhibit low potency and low affinity for cell-surface IFNAR and the poxvirus antagonist B18R. J Biol Chem. 2018;293(41):16057-68.
6. Li S-f, Zhao F-r, Shao J-j, Xie Y-l, Chang H-y and Zhang Y-g. Interferon-omega: Current status in clinical applications. Int Immunopharmacol. 2017;52):253-60.
7. Kak G, Raza M and Tiwari BK. Interferon-gamma (IFN-γ): exploring its implications in infectious diseases. Biomol Concepts. 2018;9(1):64-79.
8. Hemann EA, Gale Jr M and Savan R. Interferon lambda genetics and biology in regulation of viral control. Front Immunol. 2017;8):1707.
9. Schneider WM, Chevillotte MD and Rice CM. Interferon-stimulated genes: a complex web of host defenses. Annu Rev Immunol. 2014;32):513-45.
10. Kotenko SV and Durbin JE. Contribution of type III interferons to antiviral immunity: location, location, location. J Biol Chem. 2017;292(18):7295-303.
11. Fensterl V and Sen GC. Interferons and viral infections. Biofactors. 2009;35(1):14-20.
12. Lazear HM, Schoggins JW and Diamond MS. Shared and distinct functions of type I and type III interferons. Immunity. 2019;50(4):907-23.
13. Takaoka A and Yanai H. Interferon signalling network in innate defence. Cell Microbiol. 2006;8(6):907-22.
14. Stark GR and Darnell Jr JE. The JAK-STAT pathway at twenty. Immunity. 2012;36(4):503-14.
15. Schoggins JW. Interferon-stimulated genes: what do they all do? Annu Rev Virol. 2019;6):567-84.
16. Aso H, Ito J, Koyanagi Y and Sato K. Comparative description of the expression profile of interferon-stimulated genes in multiple cell lineages targeted by HIV-1 infection. Front Microbiol. 2019;10):429.
17. Dang W, Xu L, Yin Y, Chen S, Wang W, Hakim MS, et al. IRF-1, RIG-I and MDA5 display potent antiviral activities against norovirus coordinately induced by different types of interferons. Antiviral Res. 2018;155):48-59.
18. Masola V, Bellin G, Gambaro G and Onisto M. Heparanase: A multitasking protein involved in extracellular matrix (ECM) remodeling and intracellular events. Cells. 2018;7(12):236.
19. Schoggins JW. Recent advances in antiviral interferon-stimulated gene biology. F1000Research. 2018;7

20. Spence JS, He R, Hoffmann H-H, Das T, Thinon E, Rice CM, et al. IFITM3 directly engages and shuttles incoming virus particles to lysosomes. Nat Chem Biol. 2019;15(3):259-68.
21. Haller O, Staeheli P, Schwemmle M and Kochs G. Mx GTPases: dynamin-like antiviral machines of innate immunity. Trends Microbiol. 2015;23(3):154-63.
22. García-Sastre A. Ten strategies of interferon evasion by viruses. Cell Host Microbe. 2017;22(2):176-84.
23. Giotis ES, Robey RC, Skinner NG, Tomlinson CD, Goodbourn S and Skinner MA. Chicken interferome: avian interferon-stimulated genes identified by microarray and RNA-seq of primary chick embryo fibroblasts treated with a chicken type I interferon (IFN-α). Vet Res. 2016;47(1):1-12.
24. Rusinova I, Forster S, Yu S, Kannan A, Masse M, Cumming H, et al. Interferome v2. 0: an updated database of annotated interferon-regulated genes. Nucleic Acids Res. 2012;41(D1):D1040-D6.
25. OhAinle M, Helms L, Vermeire J, Roesch F, Humes D, Basom R, et al. A virus-packageable CRISPR screen identifies host factors mediating interferon inhibition of HIV. Elife. 2018;7):e39823.
26. Zhang Y, Burke CW, Ryman KD and Klimstra WB. Identification and characterization of interferon-induced proteins that inhibit alphavirus replication. J Virol. 2007;81(20):11246-55.
27. Stark R, Grzelak M and Hadfield J. RNA sequencing: the teenage years. Nature Reviews Genetics. 2019;20(11):631-56.
28. Pamela C, Kanchwala M, Liang H, Kumar A, Wang L-F, Xing C, et al. The IFN response in bats displays distinctive IFN-stimulated gene expression kinetics with atypical RNASEL induction. The Journal of Immunology. 2018;200(1):209-17.
29. Feld JJ, Nanda S, Huang Y, Chen W, Cam M, Pusek SN, et al. Hepatic gene expression during treatment with peginterferon and ribavirin: Identifying molecular pathways for treatment response. Hepatology. 2007;46(5):1548-63.
30. Dalman MR, Deeter A, Nimishakavi G and Duan Z-H. Fold change and p-value cutoffs significantly alter microarray interpretations. In: *BMC Bioinformatics* 2012, pp.1-4. BioMed Central.
31. Trilling M, Bellora N, Rutkowski AJ, de Graaf M, Dickinson P, Robertson K, et al. Deciphering the modulation of gene expression by type I and II interferons combining 4sU-tagging, translational arrest and in silico promoter analysis. Nucleic Acids Res. 2013;41(17):8107-25.
32. O'Leary NA, Wright MW, Brister JR, Ciufo S, Haddad D, McVeigh R, et al. Reference sequence (RefSeq) database at NCBI: current status, taxonomic expansion, and functional annotation. Nucleic Acids Res. 2016;44(D1):D733-D45.
33. Bragg JG, Potter S, Bi K and Moritz C. Exon capture phylogenomics: efficacy across scales of divergence. Mol Ecol Resour. 2016;16(5):1059-68.
34. Kondrashov FA, Rogozin IB, Wolf YI and Koonin EV. Selection in the evolution of gene duplications. Genome Biol. 2002;3(2):1-9.
35. Esposito M and Moreno-Hagelsieb G. Non-synonymous to synonymous substitutions suggest that orthologs tend to keep their functions, while paralogs are a source of functional novelty. bioRxiv. 2018):354704.
36. MacFarland TW and Yates JM. Mann–whitney u test. Introduction to nonparametric statistics for the biological sciences using R. Springer; 2016. p. 103-32.
37. Van den Eynden J and Larsson E. Mutational signatures are critical for proper estimation of purifying selection pressures in cancer somatic mutation data when using the dN/dS metric. Front Genet. 2017;8):74.

38. Song H, Bremer BJ, Hinds EC, Raskutti G and Romero PA. Inferring protein sequence-function relationships with large-scale positive-unlabeled learning. Cell Syst. 2020;
39. Pessia E, Popa A, Mousset S, Rezvoy C, Duret L and Marais GA. Evidence for widespread GC-biased gene conversion in eukaryotes. Genome Biol Evol. 2012;4(7):675-82.
40. Zhou Z, Dang Y, Zhou M, Li L, Yu C-h, Fu J, et al. Codon usage is an important determinant of gene expression levels largely through its effects on transcription. Proceedings of the National Academy of Sciences. 2016;113(41):E6117-E25.
41. Sievers A, Bosiek K, Bisch M, Dreessen C, Riedel J, Froß P, et al. K-mer content, correlation, and position analysis of genome DNA sequences for the identification of function and evolutionary features. Genes. 2017;8(4):122.
42. Lee NK, Li X and Wang D. A comprehensive survey on genetic algorithms for DNA motif prediction. Inf Sci. 2018;466):25-43.
43. Noble WS. How does multiple testing correction work? Nat Biotechnol. 2009;27(12):1135-7.
44. Di Rienzo L, Miotto M, Bò L, Ruocco G, Raimondo D and Milanetti E. Characterizing hydropathy of amino acid side chain in a protein environment by investigating the structural changes of water molecules network. Front Mol Biosci. 2021;8
45. Bhadra P, Yan J, Li J, Fong S and Siu SW. AmPEP: Sequence-based prediction of antimicrobial peptides using distribution patterns of amino acid properties and random forest. Sci Rep. 2018;8(1):1-10.
46. Pommié C, Levadoux S, Sabatier R, Lefranc G and Lefranc MP. IMGT standardized criteria for statistical analysis of immunoglobulin V- REGION amino acid properties. J Mol Recognit. 2004;17(1):17-32.
47. Kumar M, Gouw M, Michael S, Sámano-Sánchez H, Pancsa R, Glavina J, et al. ELM—the eukaryotic linear motif resource in 2020. Nucleic Acids Res. 2020;48(D1):D296-D306.
48. Pfleger CM and Kirschner MW. The KEN box: an APC recognition signal distinct from the D box targeted by Cdh1. Genes Dev. 2000;14(6):655-65.
49. Fehr AR and Yu D. Control the host cell cycle: viral regulation of the anaphase-promoting complex. J Virol. 2013;87(16):8818-25.
50. Bösl K, Ianevski A, Than TT, Andersen PI, Kuivanen S, Teppor M, et al. Common nodes of virus–host interaction revealed through an integrated network analysis. Front Immunol. 2019;10):2186.
51. Wright PE and Dyson HJ. Intrinsically disordered proteins in cellular signalling and regulation. Nat Rev Mol Cell Biol. 2015;16(1):18-29.
52. Mészáros B, Erdős G and Dosztányi Z. IUPred2A: context-dependent prediction of protein disorder as a function of redox state and protein binding. Nucleic Acids Res. 2018;46(W1):W329-W37.
53. Hagai T, Azia A, Babu MM and Andino R. Use of host-like peptide motifs in viral proteins is a prevalent strategy in host-virus interactions. Cell Rep. 2014;7(5):1729-39.
54. Michael S, Travé G, Ramu C, Chica C and Gibson TJ. Discovery of candidate KEN-box motifs using cell cycle keyword enrichment combined with native disorder prediction and motif conservation. Bioinformatics. 2008;24(4):453-7.
55. Alanis-Lobato G, Andrade-Navarro MA and Schaefer MH. HIPPIE v2.0: enhancing meaningfulness and reliability of protein–protein interaction networks. Nucleic Acids Res. 2016):gkw985.
56. Abedi M and Gheisari Y. Nodes with high centrality in protein interaction networks are responsible for driving signaling pathways in diabetic nephropathy. PeerJ. 2015;3):e1284.

57. Ozato K, Shin D-M, Chang T-H and Morse HC. TRIM family proteins and their emerging roles in innate immunity. Nat Rev Immunol. 2008;8(11):849-60.
58. Yates AD, Achuthan P, Akanni W, Allen J, Allen J, Alvarez-Jarreta J, et al. Ensembl 2020. Nucleic Acids Res. 2020;48(D1):D682-D8.
59. Shaw AE, Rihn SJ, Mollentze N, Wickenhagen A, Stewart DG, Orton RJ, et al. The antiviral state has shaped the CpG composition of the vertebrate interferome to avoid self-targeting. PLoS Biol. 2021;19(9):e3001352.
60. Zhang M-L and Zhou Z-H. ML-KNN: A lazy learning approach to multi-label learning. Pattern recognition. 2007;40(7):2038-48.
61. Chang C-C and Lin C-J. LIBSVM: A library for support vector machines. ACM Trans Intell Syst Technol. 2011;2(3):1-27.
62. Sivaranjani S, Ananya S, Aravinth J and Karthika R. Diabetes prediction using machine learning algorithms with feature selection and dimensionality reduction. In: *2021 7th International Conference on Advanced Computing and Communication Systems (ICACCS)* 2021, pp.141-6. IEEE.
63. Cheng D, Zhang S, Deng Z, Zhu Y and Zong M. kNN algorithm with data-driven k value. In: *International Conference on Advanced Data Mining and Applications* 2014, pp.499-512. Springer.
64. Liu X-Y, Wu J and Zhou Z-H. Exploratory undersampling for class-imbalance learning. IEEE Trans Syst Man Cybern. 2008;39(2):539-50.
65. Lonsdale J, Thomas J, Salvatore M, Phillips R, Lo E, Shad S, et al. The genotype-tissue expression (GTEx) project. Nat Genet. 2013;45(6):580-5.
66. Papatheodorou I, Moreno P, Manning J, Fuentes AM-P, George N, Fexova S, et al. Expression Atlas update: from tissues to single cells. Nucleic Acids Res. 2020;48(D1):D77-D83.
67. Jeong H, Mason SP, Barabási A-L and Oltvai ZN. Lethality and centrality in protein networks. Nature. 2001;411(6833):41-2.
68. Hahn MW and Kern AD. Comparative genomics of centrality and essentiality in three eukaryotic protein-interaction networks. Mol Biol Evol. 2005;22(4):803-6.
69. Batada NN, Hurst LD and Tyers M. Evolutionary and physiological importance of hub proteins. PLoS Comput Biol. 2006;2(7):e88.
70. Pérez-Martínez D. Innate immunity in vertebrates: an overview. Immunology. 2016;148(2):125-39.
71. Jopling CL. Mutations: Stop that nonsense! Elife. 2014;3):e04300.
72. Zhu X, Pribis JP, Rodriguez PC, Morris Jr SM, Vodovotz Y, Billiar TR, et al. The central role of arginine catabolism in T-cell dysfunction and increased susceptibility to infection after physical injury. Ann Surg. 2014;259(1):171-8.
73. Morris CR, Hamilton- Reeves J, Martindale RG, Sarav M and Ochoa Gautier JB. Acquired amino acid deficiencies: a focus on arginine and glutamine. Nutr Clin Pract. 2017;32):30S-47S.
74. Levring TB, Hansen AK, Nielsen BL, Kongsbak M, Von Essen MR, Woetmann A, et al. Activated human CD4+ T cells express transporters for both cysteine and cystine. Sci Rep. 2012;2(1):1-6.
75. Sikalidis AK. Amino acids and immune response: a role for cysteine, glutamine, phenylalanine, tryptophan and arginine in T-cell function and cancer? Pathol Oncol Res. 2015;21(1):9-17.
76. Yin C, Zheng T and Chang X. Biosynthesis of S-Adenosylmethionine by magnetically immobilized Escherichia coli cells highly expressing a methionine adenosyltransferase variant. Molecules. 2017;22(8):1365.

77. Feld JJ, Modi AA, El–Diwany R, Rotman Y, Thomas E, Ahlenstiel G, et al. S-adenosyl methionine improves early viral responses and interferon-stimulated gene induction in hepatitis C nonresponders. Gastroenterology. 2011;140(3):830-9.
78. Yeom S, Giacomelli I, Fredrikson M and Jha S. Privacy risk in machine learning: Analyzing the connection to overfitting. In: *2018 IEEE 31st Computer Security Foundations Symposium (CSF)* 2018, pp.268-82. IEEE.
79. Li S-W, Lai C-C, Ping J-F, Tsai F-J, Wan L, Lin Y-J, et al. Severe acute respiratory syndrome coronavirus papain-like protease suppressed alpha interferon-induced responses through downregulation of extracellular signal-regulated kinase 1-mediated signalling pathways. J Gen Virol. 2011;92(5):1127-40.
80. Flo TH, Smith KD, Sato S, Rodriguez DJ, Holmes MA, Strong RK, et al. Lipocalin 2 mediates an innate immune response to bacterial infection by sequestrating iron. Nature. 2004;432(7019):917-21.
81. Tissot C, Rebouissou C, Klein B and Mechti N. Both human α/β and γ interferons upregulate the expression of CD48 cell surface molecules. J Interferon Cytokine Res. 1997;17(1):17-26.
82. Noçon AL, Ip JP, Terry R, Lim SL, Getts DR, Müller M, et al. The bacteriostatic protein lipocalin 2 is induced in the central nervous system of mice with West Nile virus encephalitis. J Virol. 2014;88(1):679-89.
83. Zarama A, Perez-Carmona N, Farre D, Tomic A, Borst EM, Messerle M, et al. Cytomegalovirus m154 hinders CD48 cell-surface expression and promotes viral escape from host natural killer cell control. PLoS Pathog. 2014;10(3):e1004000.
84. Martínez-Vicente P, Farré D, Engel P and Angulo A. Divergent Traits and Ligand-Binding Properties of the Cytomegalovirus CD48 Gene Family. Viruses. 2020;12(8):813.
85. Ricquier D. UCP1, the mitochondrial uncoupling protein of brown adipocyte: a personal contribution and a historical perspective. Biochimie. 2017;134):3-8.
86. Hossain MA, Larrous F, Rawlinson SM, Zhan J, Sethi A, Ibrahim Y, et al. Structural elucidation of viral antagonism of innate immunity at the STAT1 interface. Cell Rep. 2019;29(7):1934-45. e8.
87. Yu X, Liu H, Hamel KA, Morvan MG, Yu S, Leff J, et al. Dorsal root ganglion macrophages contribute to both the initiation and persistence of neuropathic pain. Nat Commun. 2020;11(1):1-12.
88. Chen Y, Lun AT and Smyth GK. From reads to genes to pathways: differential expression analysis of RNA-Seq experiments using Rsubread and the edgeR quasi-likelihood pipeline. F1000Research. 2016;5
89. Herrero J, Muffato M, Beal K, Fitzgerald S, Gordon L, Pignatelli M, et al. Ensembl comparative genomics resources. Database. 2016;2016):bav096.
90. Li HD, Menon R, Omenn GS and Guan Y. Revisiting the identification of canonical splice isoforms through integration of functional genomics and proteomics evidence. Proteomics. 2014;14(23-24):2709-18.
91. Wang ET, Sandberg R, Luo S, Khrebtukova I, Zhang L, Mayr C, et al. Alternative isoform regulation in human tissue transcriptomes. Nature. 2008;456(7221):470-6.
92. Sieber P, Platzer M and Schuster S. The definition of open reading frame revisited. Trends Genet. 2018;34(3):167-70.
93. Pan Q, Shai O, Lee LJ, Frey BJ and Blencowe BJ. Deep surveying of alternative splicing complexity in the human transcriptome by high-throughput sequencing. Nat Genet. 2008;40(12):1413-5.

94. Guéguen L and Duret L. Unbiased estimate of synonymous and nonsynonymous substitution rates with nonstationary base composition. Mol Biol Evol. 2018;35(3):734-42.
95. Takata MA, Gonçalves-Carneiro D, Zang TM, Soll SJ, York A, Blanco-Melo D, et al. CG dinucleotide suppression enables antiviral defence targeting non-self RNA. Nature. 2017;550(7674):124-7.
96. Yu C-H, Dang Y, Zhou Z, Wu C, Zhao F, Sachs MS, et al. Codon usage influences the local rate of translation elongation to regulate co-translational protein folding. Mol Cell. 2015;59(5):744-54.
97. Tufarelli C, Ahmad A, Strohbuecker S, Scotti C and Sottile V. In Silico Identification of SOX1 Post-Translational Modifications Highlights a Shared Protein Motif. 2020;
98. Yoon J, Blumer A and Lee K. An algorithm for modularity analysis of directed and weighted biological networks based on edge-betweenness centrality. Bioinformatics. 2006;22(24):3106-8.
99. Friedel CC and Zimmer R. Influence of degree correlations on network structure and stability in protein-protein interaction networks. BMC Bioinformatics. 2007;8(1):1-10.
100. Ravasz E, Somera AL, Mongru DA, Oltvai ZN and Barabási A-L. Hierarchical organization of modularity in metabolic networks. Science. 2002;297(5586):1551-5.
101. Chicco D and Jurman G. The advantages of the Matthews correlation coefficient (MCC) over F1 score and accuracy in binary classification evaluation. BMC Genomics. 2020;21(1):1-13.

Figure 1

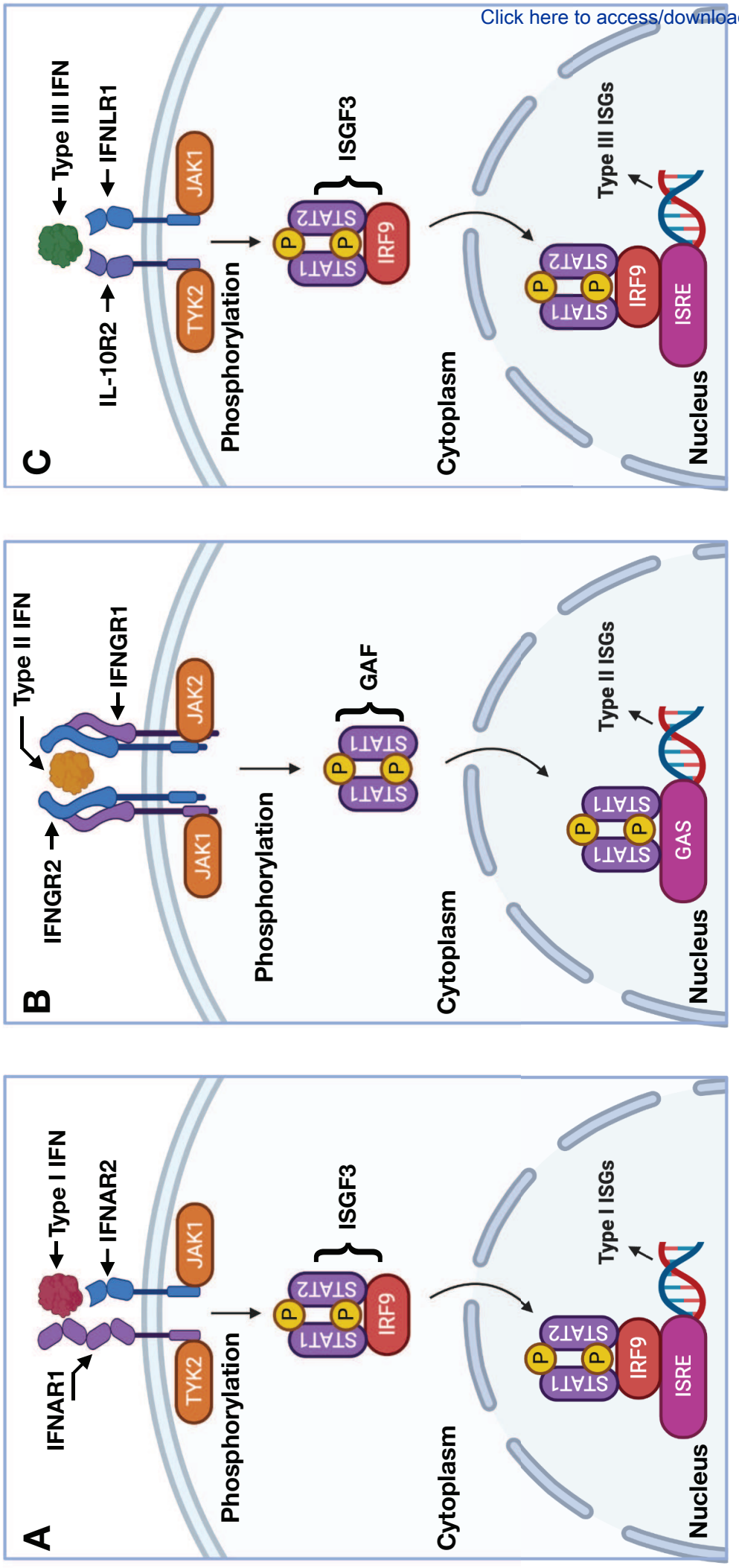

Figure 2

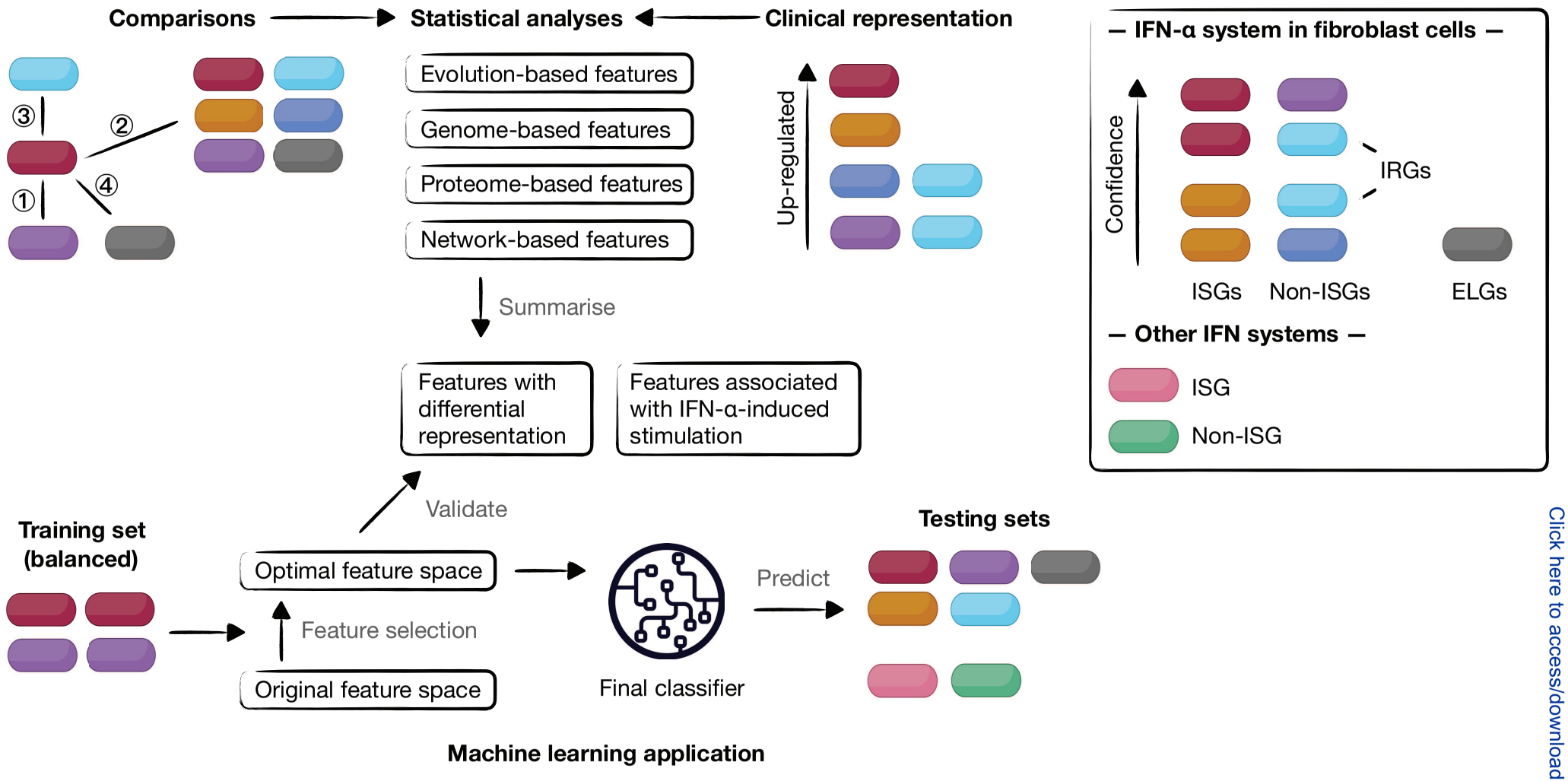

Figure 3

Click here to access/download;Figure;Figure_3.eps

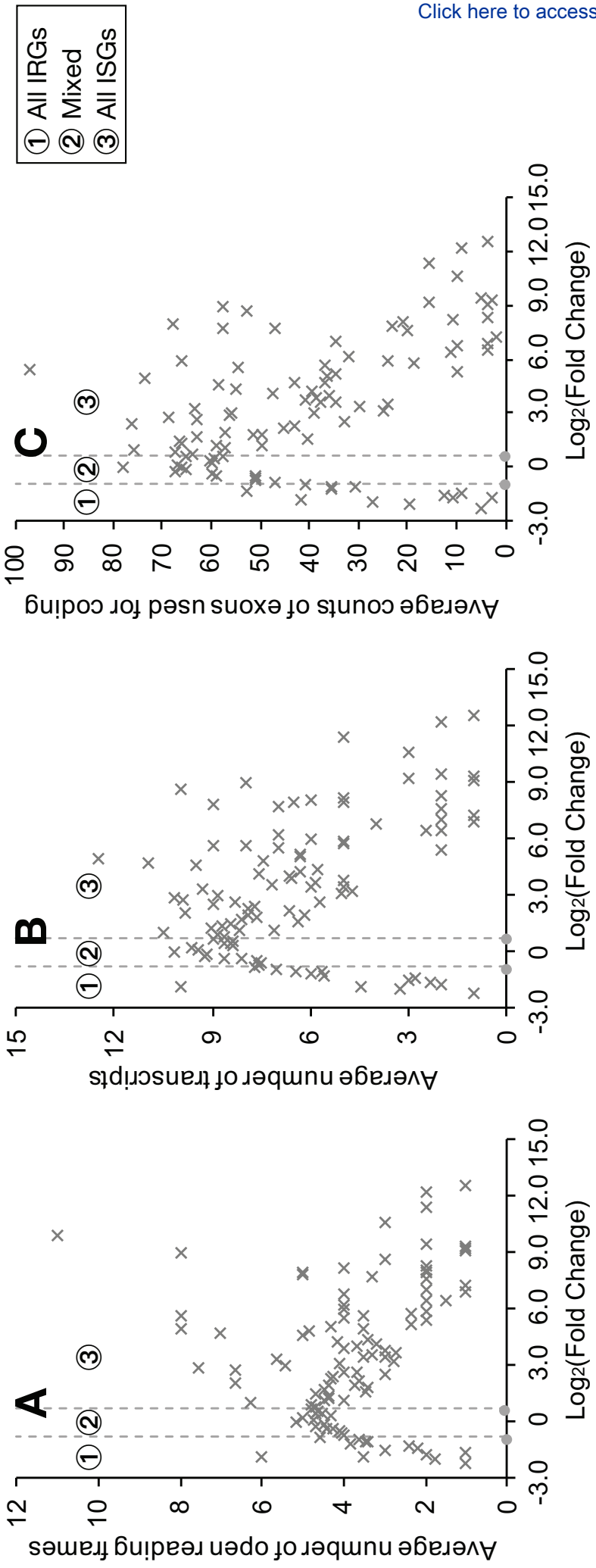

Figure 4

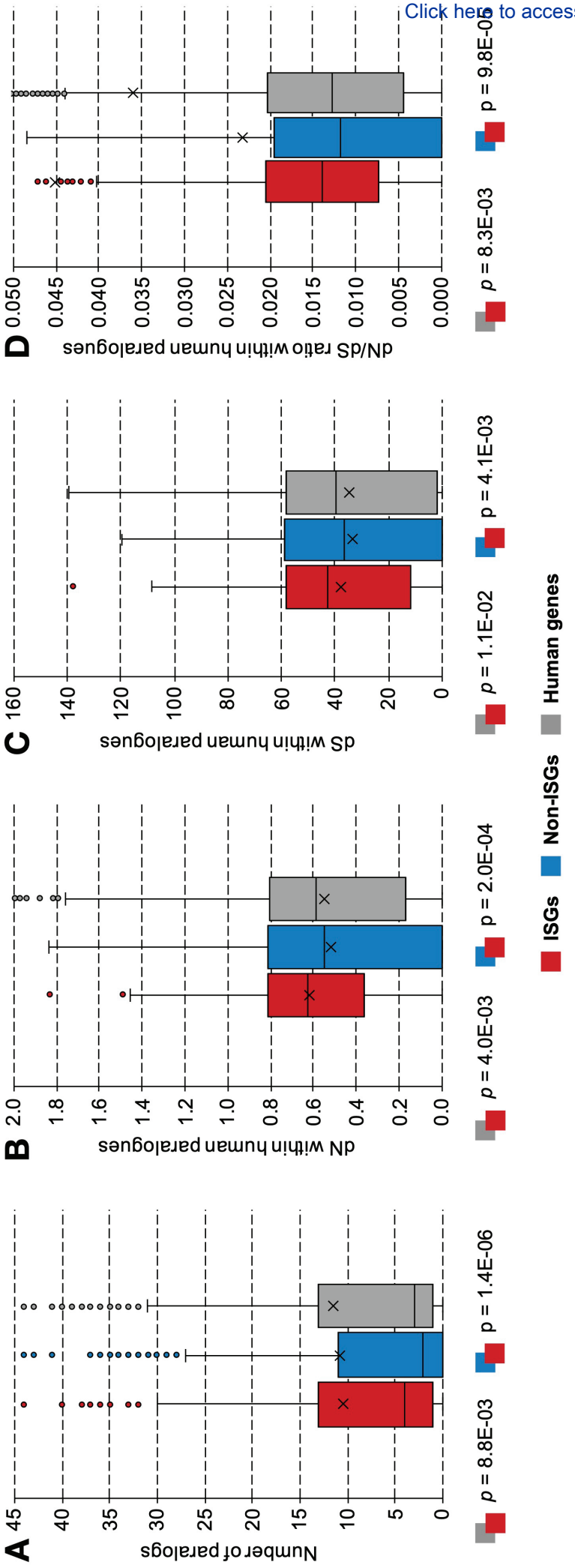

Figure 5

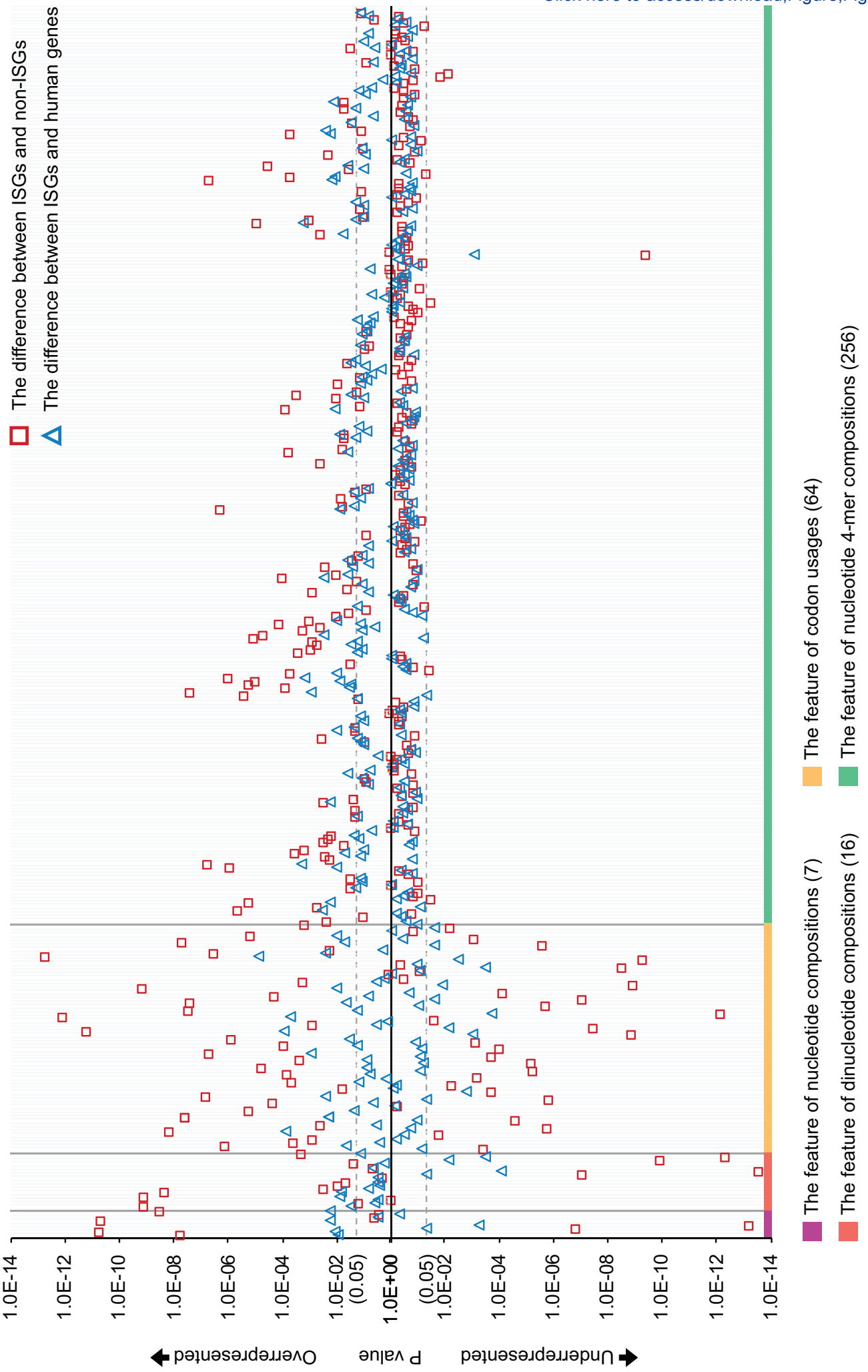

Figure 6

Click here to access/download;Figure;Figure_6.eps

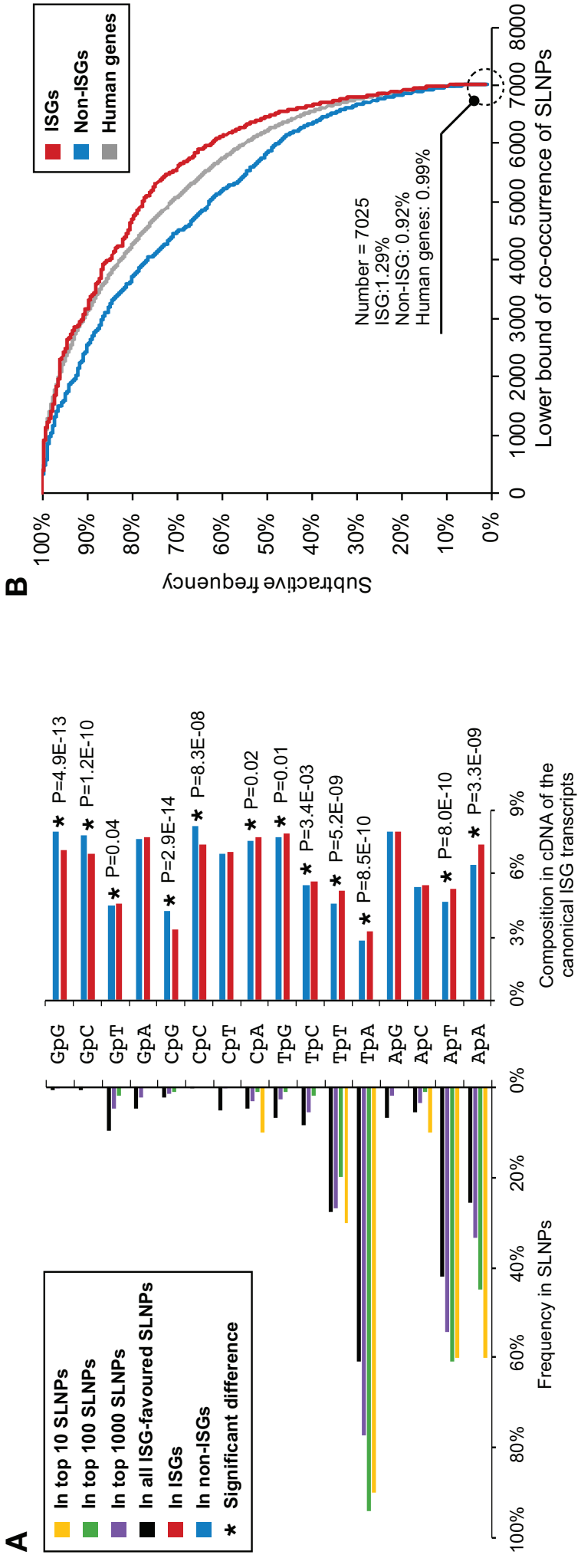

Figure 7

Click here to access/download;Figure;Figure_7.eps

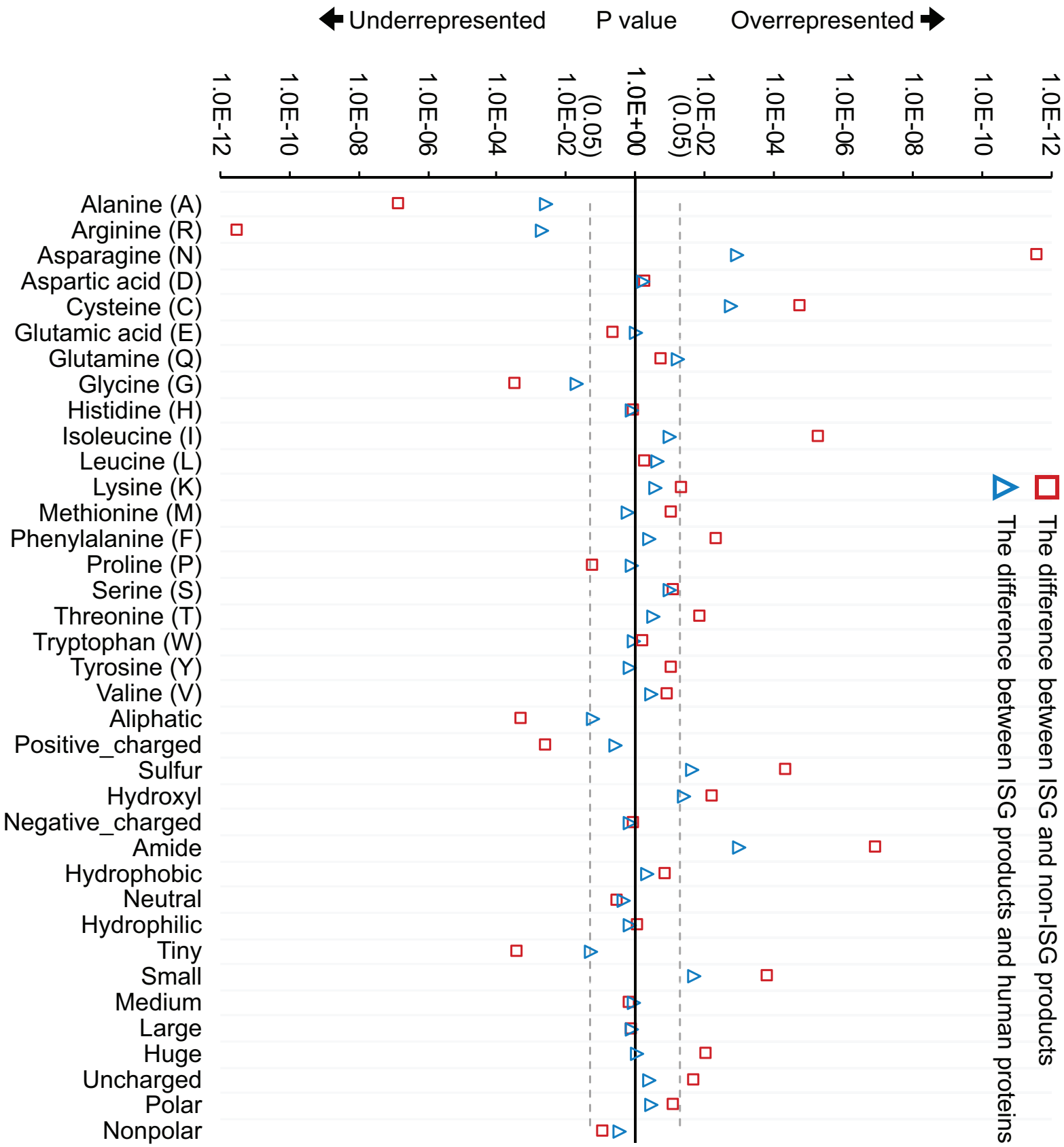

Figure 8

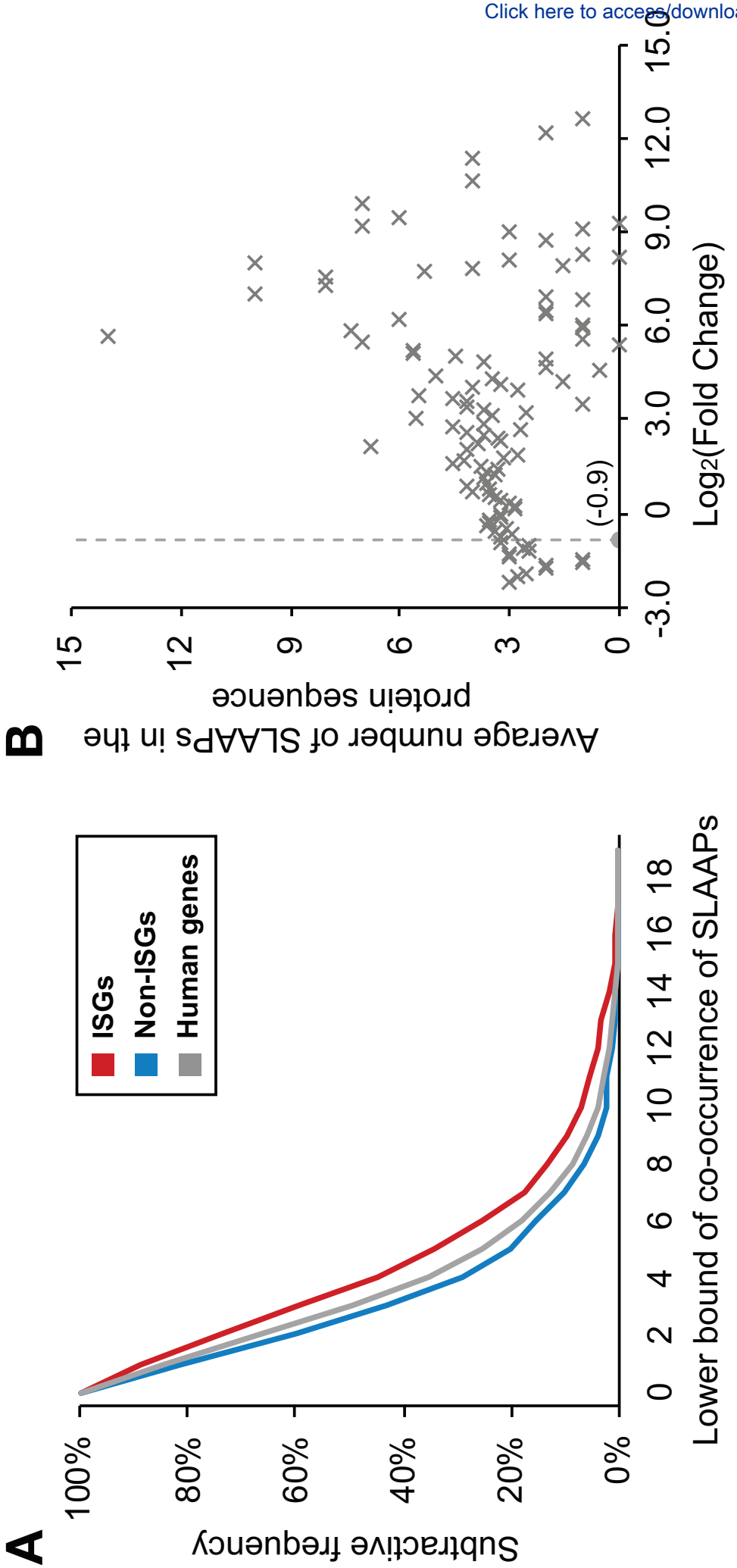

Figure 9

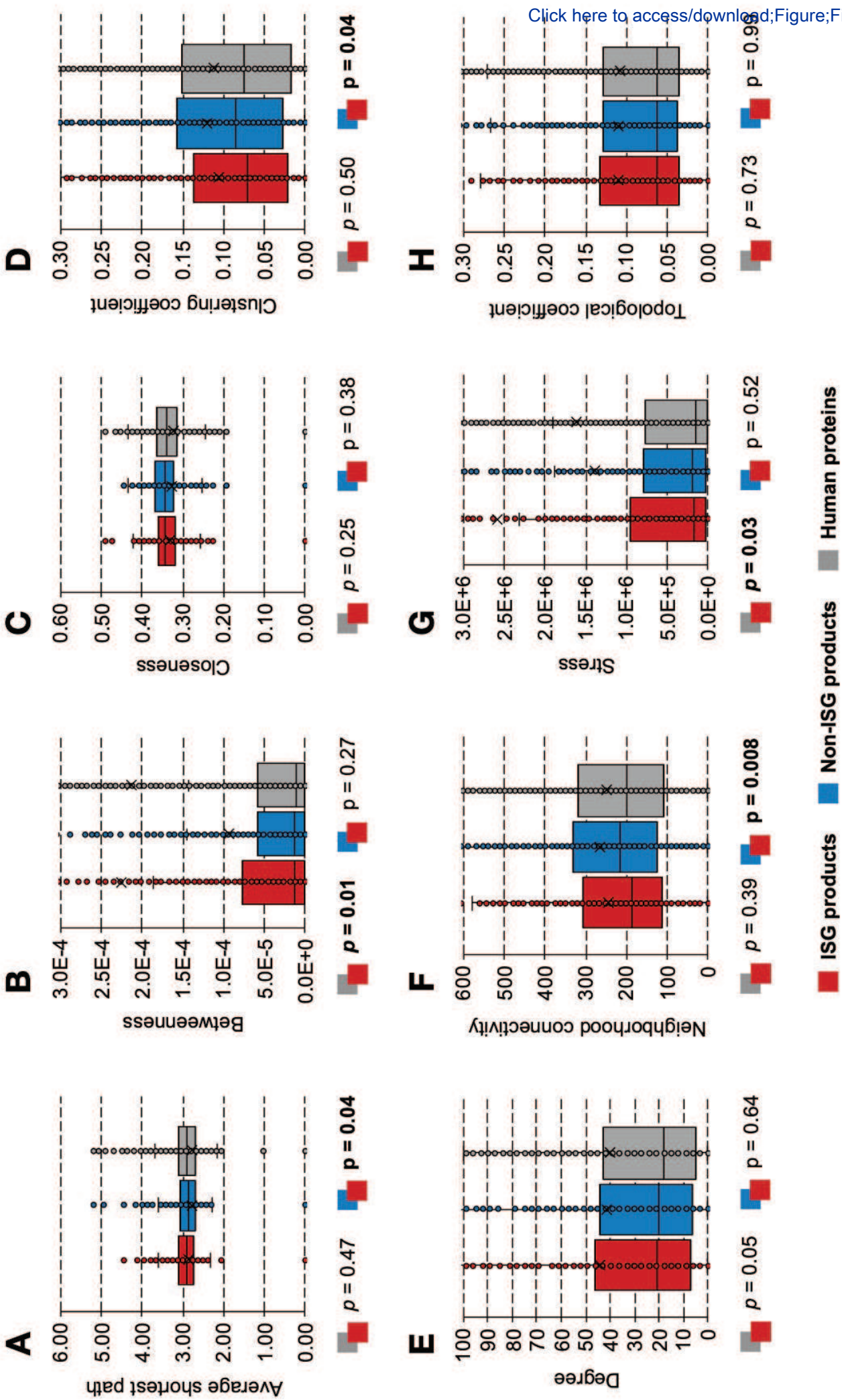

Figure 10

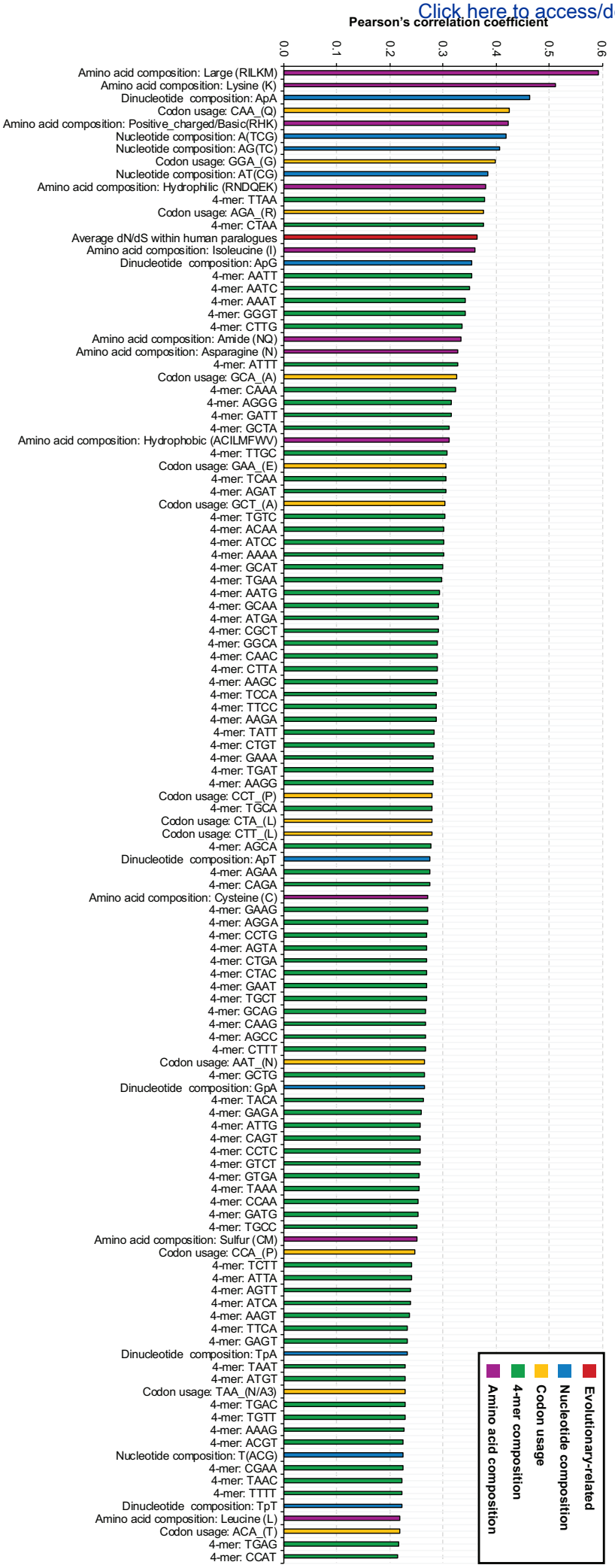

Figure 11

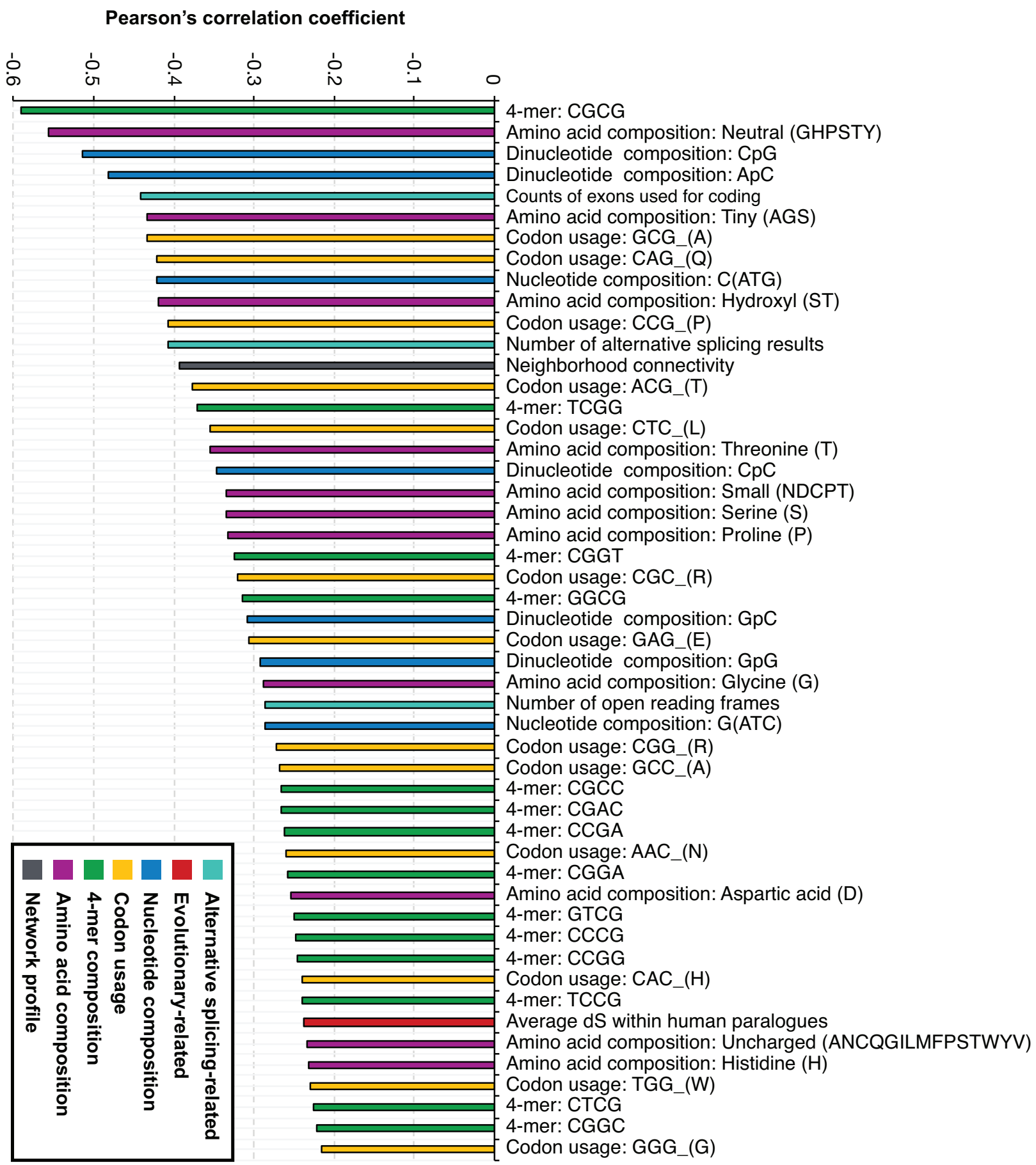

Figure 12

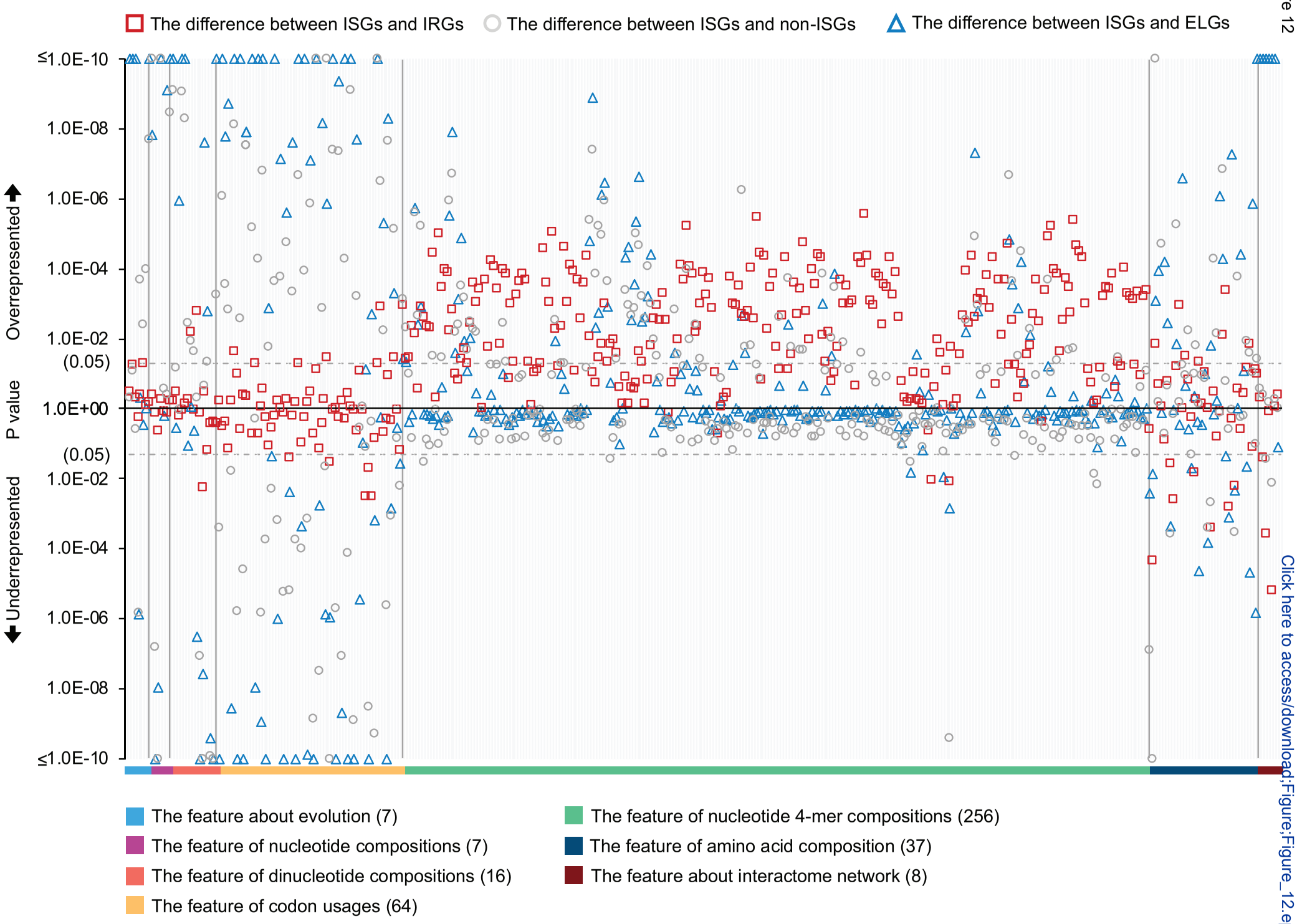

Click here to access/download;Figure;Figure_12.eps

Figure 13

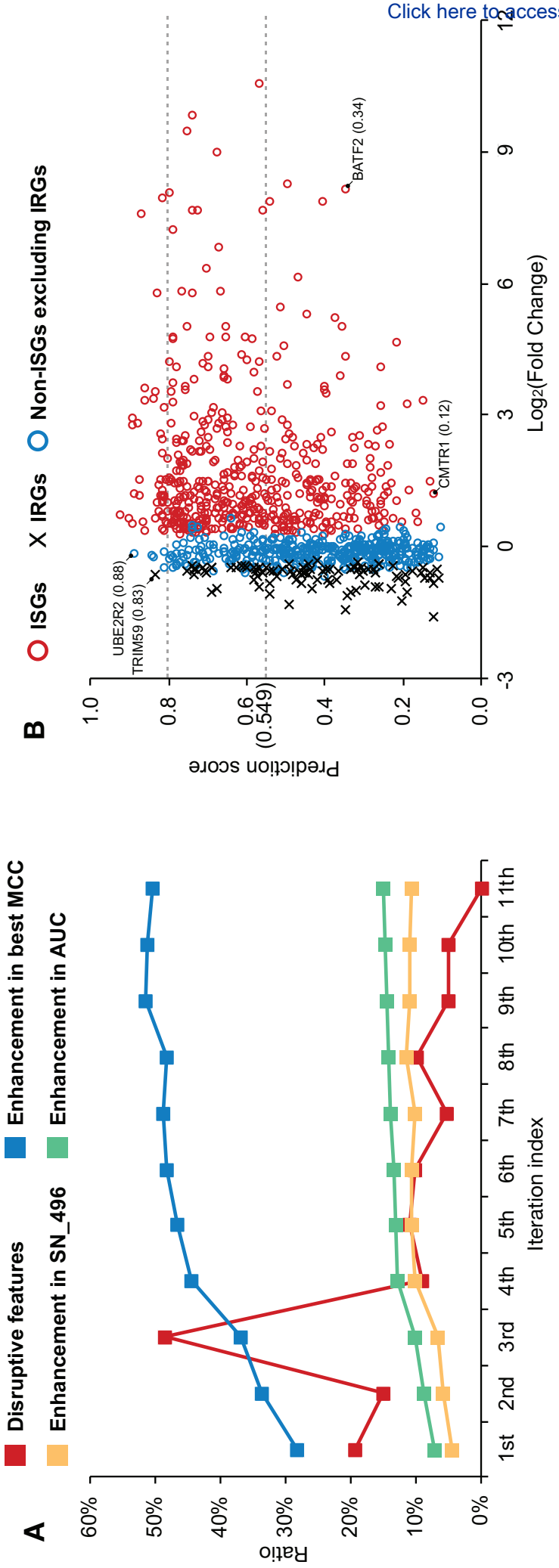

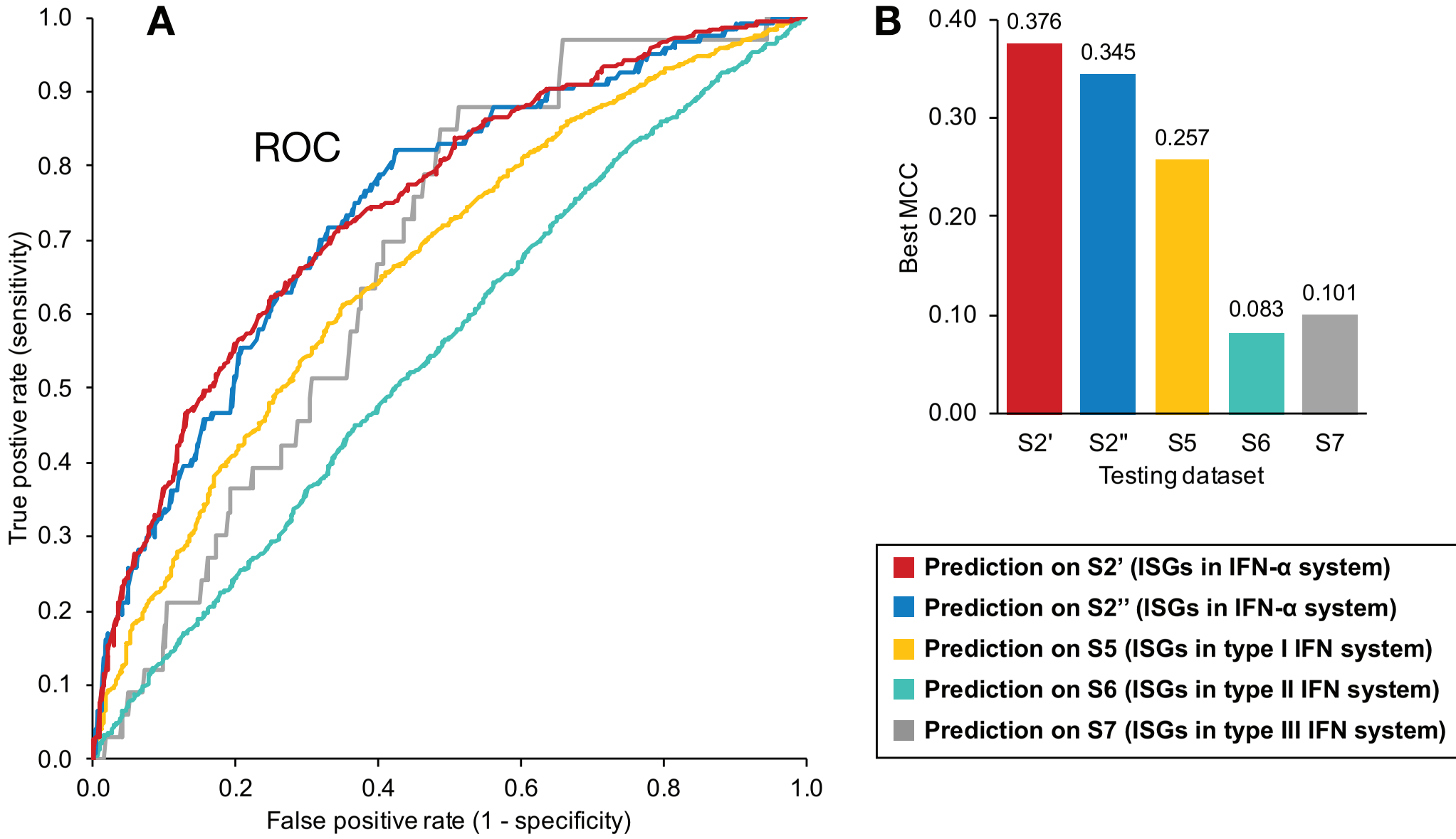

Figure 15

Click here to access/download;Figure;Figure_15.eps

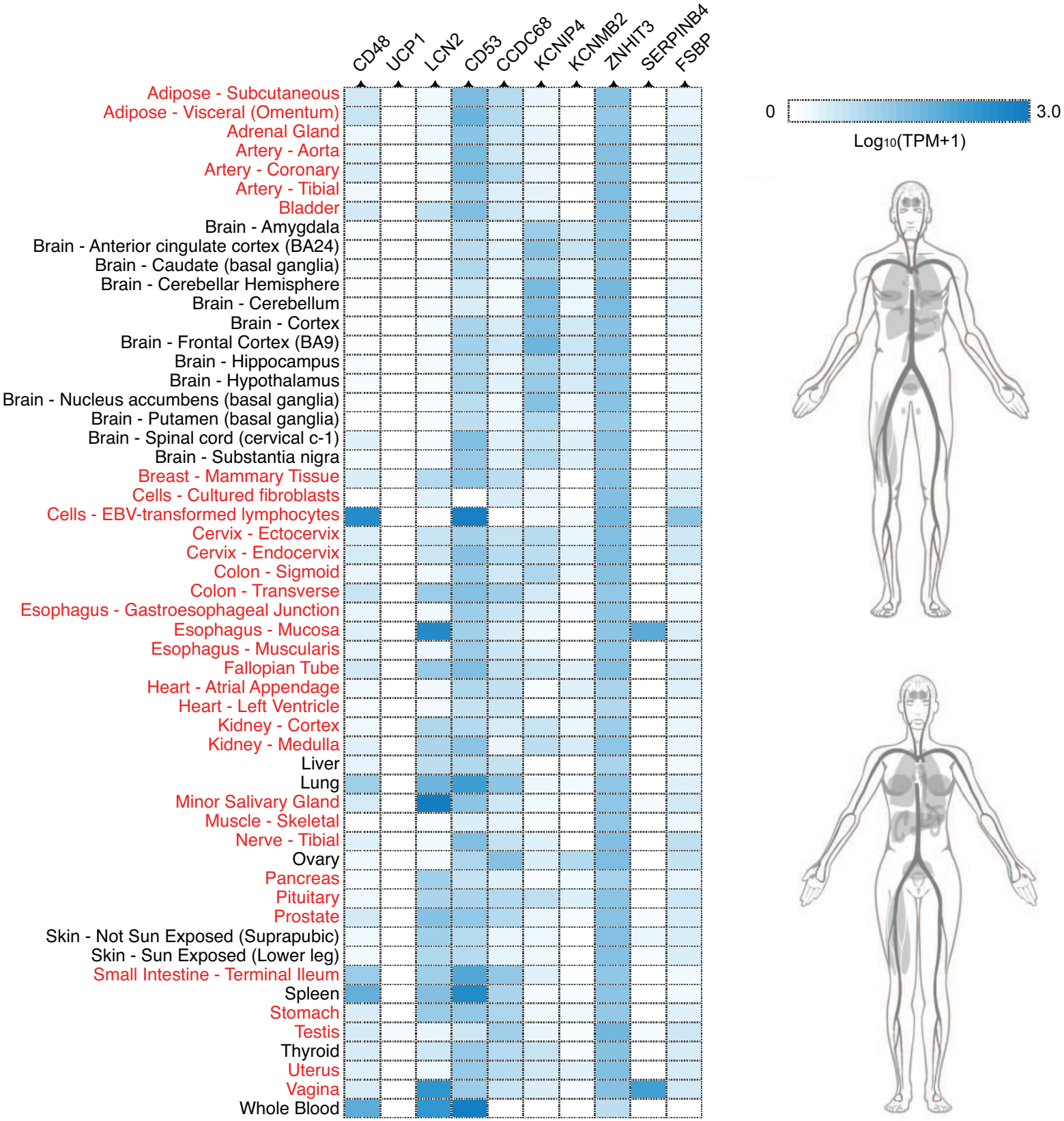

Figure 16

BEGIN

Initialisation: Balanced dataset $S_0 = \{(1, v_1^0), .. (1, v_n^0), (0, v_{n+1}^0) ... (0, v_{2n}^0)\}$, dimension of the feature vector D_0, machine learning algorithm A, number of disruptive feature $d_0 = D_0$, and iteration round $i = 0$.

While $d_0 > 0$ (i^{th} iteration):

1) Use five-fold cross validation on dataset S_i, prediction $P_i = A(S_i)$;
2) Evaluate the P_i with the criterion of AUC;
3) Remove one feature from feature vector v^i and generate a temporary dataset T_i;
4) Use five-fold cross validation on dataset T_i, prediction $P'_i = A(T_i)$;
5) Evaluate the P'_i with the criterion of AUC;
6) Repeat 4) and 5) for the traversal of D_i features;
7) Traverse v^i and remove m features helpful to improve AUC of P'_i, $d_i = m$;
8) Update dataset $S_{i+1} = \{(1, v_1^{i+1}), .. (1, v_n^{i+1}), (0, v_{n+1}^{i+1}) ... (0, v_{2n}^{i+1})\}$, $D_{i+1} = D_i - m$.

End

Output: dataset S_{i-1} encoded by D_{i-1} features.

END

Editors

GigaScience

7th September 2022

Dear Editors

On behalf of my co-authors please consider the resubmission of our research article entitled 'Defining the characteristics of interferon-alpha-stimulated human genes: insight from expression data and machine learning' for consideration in your journal. We present systematic data analyses on large-scale features to characterise the association between the response of human genes to interferons-α (IFN-α) and their inherent properties. Our results show that the up-regulated interferon-α stimulated genes (ISGs) differentially represent many features that make them distinguishable from those not significantly up-regulated (non-ISGs) in the presence of IFN-α. We find that the IFN-α repressed human genes (IRGs) have some shared properties with the ISGs. We apply machine learning ideas with an original feature selection strategy to prove the predictability of the ISGs. Our prediction method is implemented as a web server at http://isgpre.cvr.gla.ac.uk/ and Docker image at https://hub.docker.com/repository/docker/hchai01/isgpre. The source code, prediction model, and all feature profiles are released at https://github.com/HChai01/ISGPRE for reproducible use. We believe our article will be of interest to the international research community, and thus will be of interest to your readership. We confirm that this manuscript has not been published elsewhere, is not under consideration by any other journal, and that all authors have read and approved the submission of the manuscript.

Yours Sincerely,

Joseph Hughes

Medical Research Council-University of Glasgow Centre for Virus Research
Sir Michael Stoker Building, Garscube Campus, 464 Bearsden Road, Glasgow G61 1QH
cvr.ac.uk @CVRInfo